Regulation of Transcription by DNA Bending, Twisting, Looping, and Topology
Part I: In vitro approaches

Jason D. Kahn
Department of Chemistry and Biochemistry
University of Maryland, College Park

Experiments in Physical Biology

IMA, University of Minnesota

May 2-3, 2005

Kahn Lab Research

- **Design and construct interesting DNAs.**
- **Characterize their interactions with proteins: bending, twisting, writhing, looping, topology**
- **Goals:**
  - **Better methods for large-scale structure.**
  - **What are some of the structures?**
  - **Functional consequences of changes in structure?**
  - **Design new systems.**
- **Techniques:**
  - **DNA cyclization**
  - **Molecular biology: EMSA, footprinting, DNA topology**
  - **FRET, both bulk and single-molecule**
  - **Numerical simulation**

Central Dogma of Molecular Biology

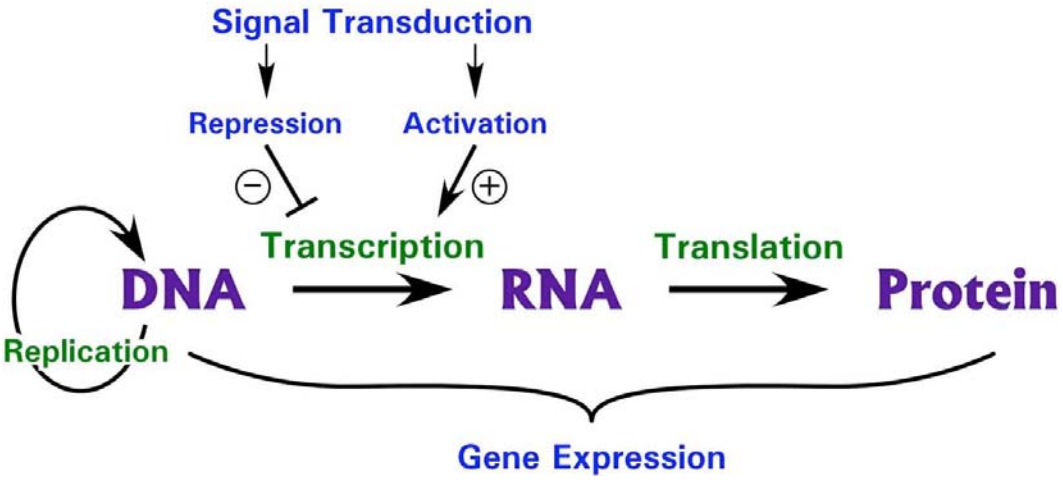

J. Kahn

DNA Cyclization Methods and Their Applications to Sequence-directed and Protein-induced DNA Bending, Twisting, Topology, and Flexibility

J. Kahn

DNA Cyclization

- DNA ring closure or cyclization requires bringing the DNA ends together, aligning the helix axes, and having the correct torsion so that 5′ and 3′ meet.
- The ring closure probability is given by the ***J* factor**, which is the effective concentration of one end of a DNA in the neighborhood of the other.
- *J* depends on DNA length, helical twist, bending, and flexibility.
- This cyclization constraints are expressed in the following equation:

$$J = 4\pi W(0)\Gamma_0(1)\Phi_{0,1}(\tau_0) / N_{AV}$$

- *W(R)* is the probability of end-to-end distance *R*, $\Gamma_0(\gamma)$ is the conditional probability that the dot product of terminal helix axes is γ, and $\Phi_{0,1}(\tau)$ is the conditional probability of torsion angle τ, where τ_0 = 360°(1-1/helical repeat)
- The *J* factor is most conveniently measured by cyclization kinetics, and flexibility and bending parameters are extracted by fitting models to the data.
- DNA minicircles (< 100 to 600 bp) are ideal systems because they are most sensitive to changes in shape and flexibility.

J. Kahn

Cyclization Kinetics Measurements and Formalism

Experiment: Compare T4 Ligase-Mediated Cyclization and Bimolecular Reactions

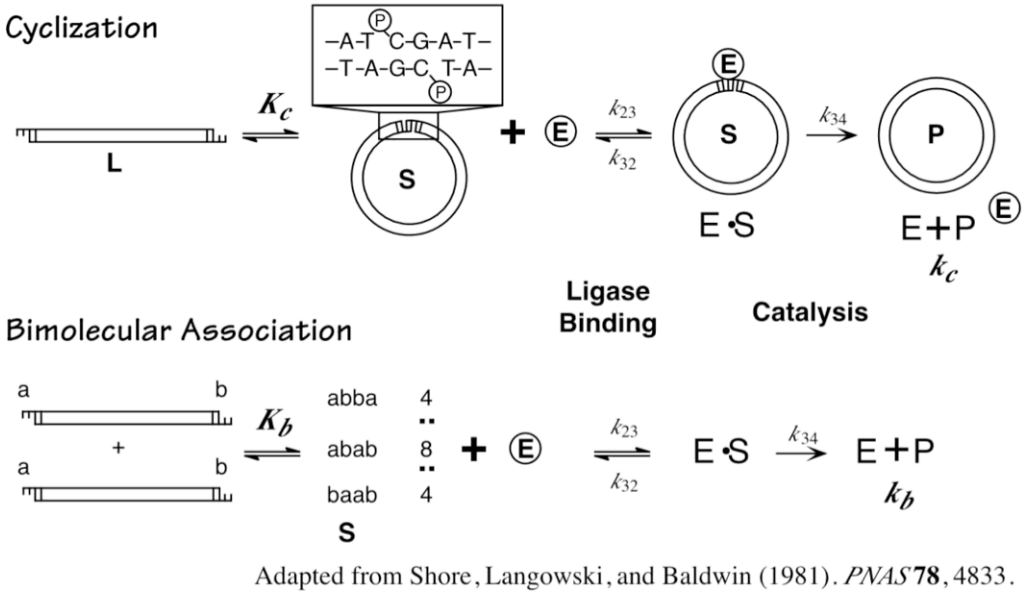

Adapted from Shore, Langowski, and Baldwin (1981). *PNAS* **78**, 4833.

J. Kahn

Shore and Baldwin Results

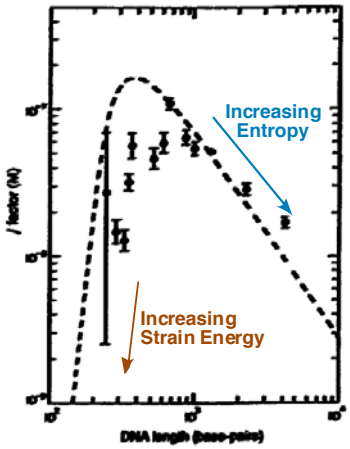

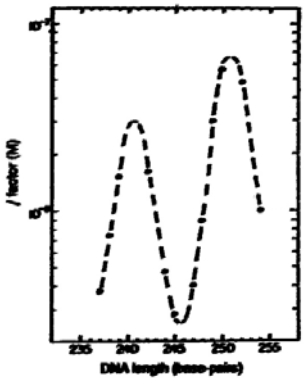

Torsional Oscillations

Figure 9-37
Cyclization probability *j* as a function of DNA length for a series of *Eco*RI restriction fragments ranging in length from (*a*) 250–4362 bp and (*b*) 237–254 bp. [Reprinted from Shore, D. and Baldwin, R. L., Twisting. I. Relation between Twist and Probability; II. Topoisomerism Analysis, *J. Mol. Biol.*, 170, 957–981, 983–1078, Copyright ©1983, by permission of the publisher Academic Press Limited London.]

From Bloomfield, Crothers, and Tinoco, 2000

J. Kahn

A-Tracts: Intrinsically Bent DNA

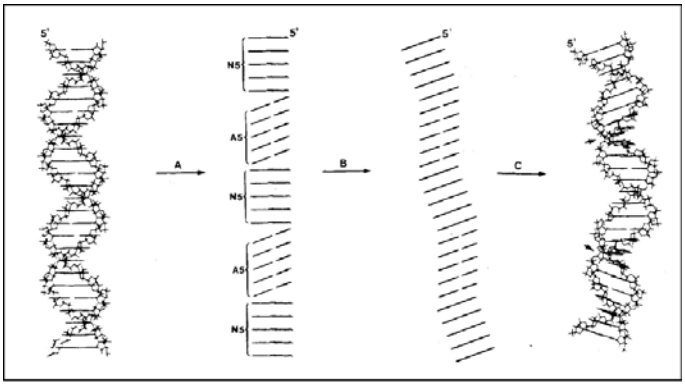

Crothers et.al. (1990). *J. Biol. Chem.*

Steps A-C are equivalent to compressing the minor groove at the centers of the A-tracts.

A-tracts repeated in phase with the helical repeat add up to give substantial DNA bends

We use them as tools.

J. Kahn

Protein Bending, DNA Cyclization and Minicircle Binding

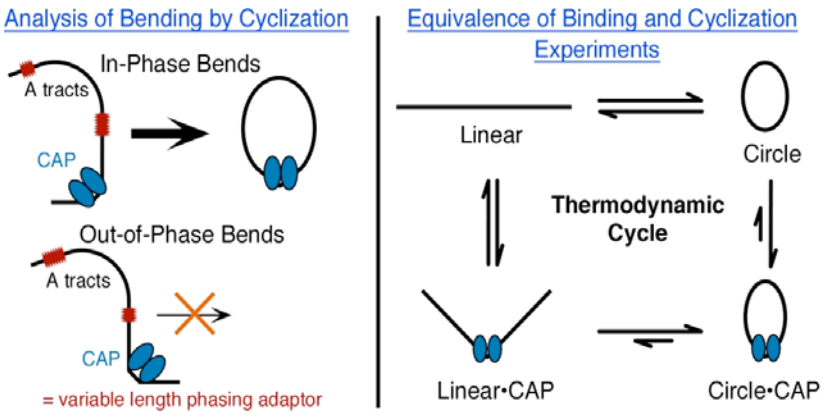

- The left panel illustrates enhanced cyclization of DNA with in-phase protein-induced and sequence-directed bends, as well as repression of cyclization caused by out-of-phase bends. Total DNA length, and therefore the torsional phasing at the ends, is independently controlled by the second phasing adaptor or by PCR.
- The right panel illustrates thermodynamic linkage between the effect of bound protein on cyclization and the effect of cyclization on protein binding: minicircle DNA is pre-bent, so protein binding is strongly enhanced. Thus cyclization kinetics and minicircle binding are equivalent experiments, and they can be used interchangeably.

J. Kahn

Demonstrating Bending-Binding Connection

Quasi-thermodynamic Cycle

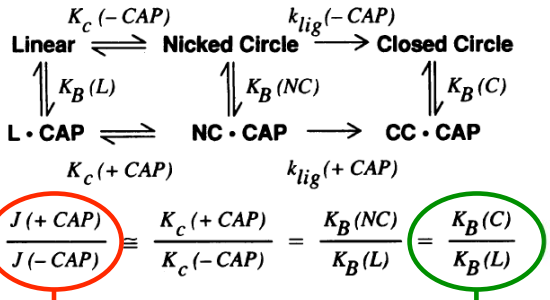

Cyclization kinetics

Gel mobility shift competition

Enhanced binding of CAP to in-phase ~150 bp minicircles

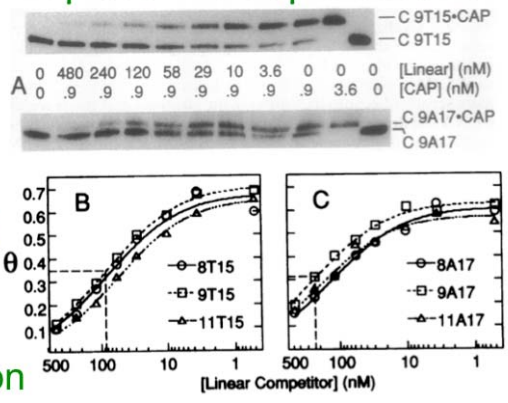

- We compare ratios of *J* factors with ratios of binding constants, find good agreement.

J. Kahn

Kahn and Crothers, PNAS 1992

Detection of DNA Flexibility

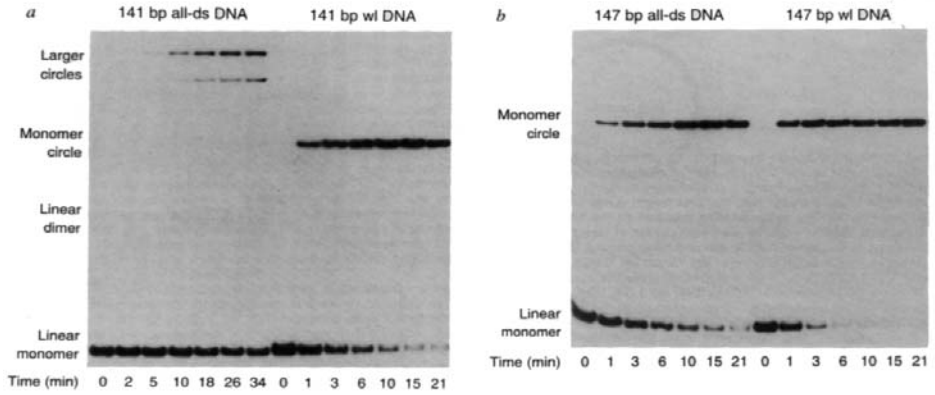

- Old data: Kahn, Yun, and Crothers 1994
- Cyclization of 141 and 147-bp DNAs with or without 3-nt interna loops
- Loop enables 141bp DNA to cyclize: torsional flexibility
- Also see weak enhancement of 147 bp cyclization: bending flexibility

J. Kahn

Kahn, Yun, and Crothers, Nature 1994

J factors for Flexible DNA

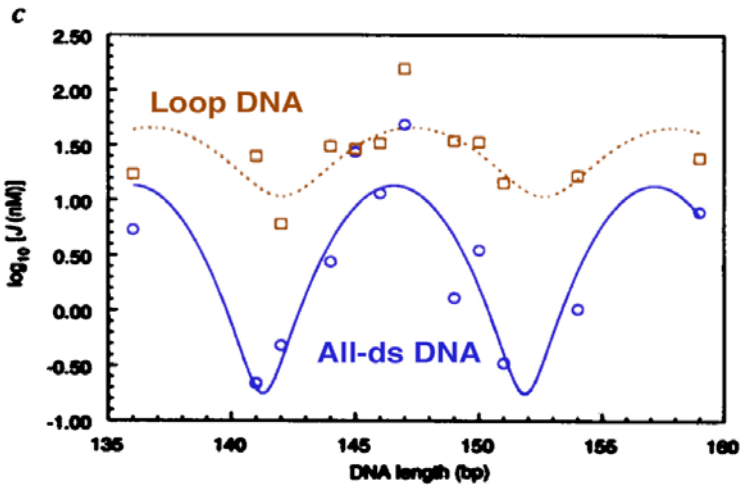

- J factors as a function of length were fit to a sum of Gaussians.
- Flattening due to torsional flexibility, elevation due to bending flexibility. No bend phasing dependence.

J. Kahn

Application of DNA Cyclization to the Solution Shape and Flexibility of TATA box DNA, TBP•DNA, and Assembled Complexes

J. Kahn

The TATA Box Binding Protein (TBP)

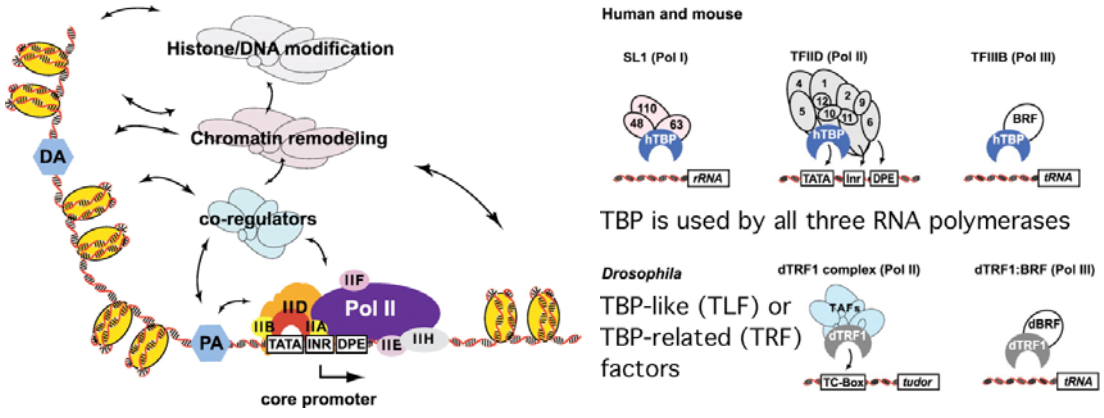

Hochheimer and Tjian, Genes Dev. 2003.

J. Kahn

DNA Deformation Induced by TBP

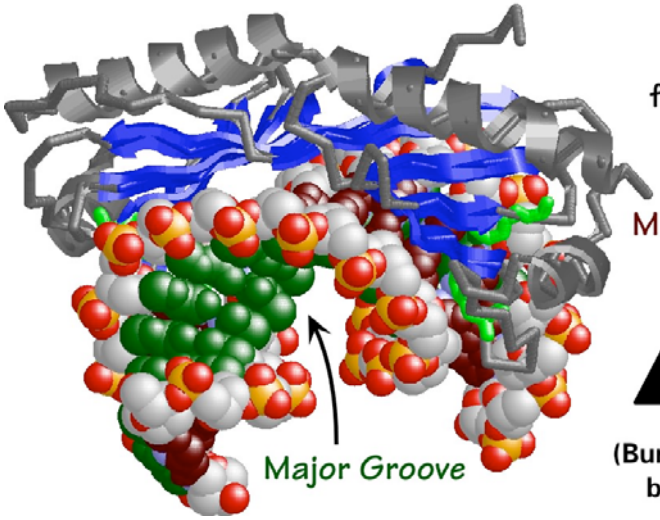

A net 80° bend (viewed from the side) comes from a contorted geometry

(Burley, Sigler; this is hTBP but they all look alike)

J. Kahn

DNA Deformation Induced by TBP

Intercalating phenylalanines are responsible for out-of-plane bending, and there is substantial bending by roll across the top of the saddle

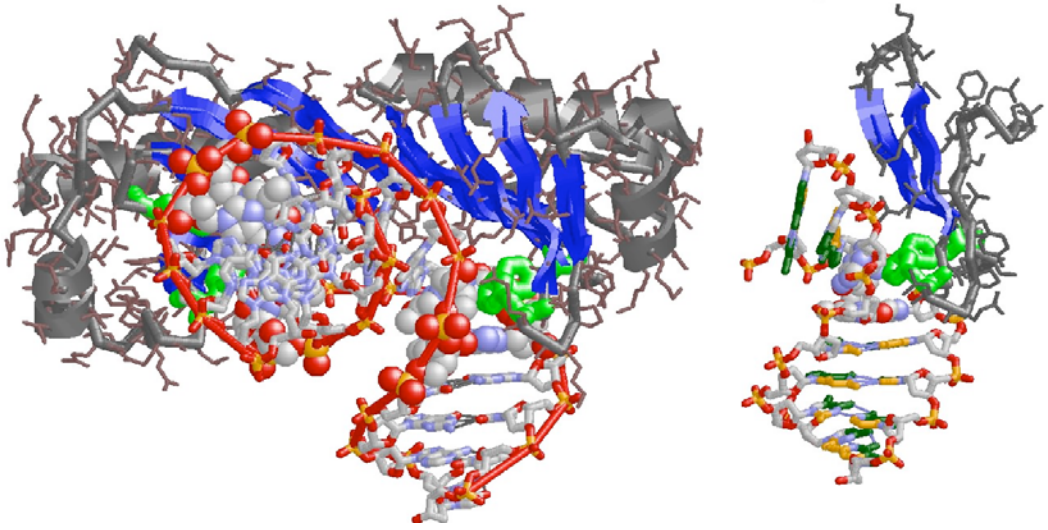

J. Kahn

Cyclization Constructs Used for Analysis of TBP-induced DNA Deformation

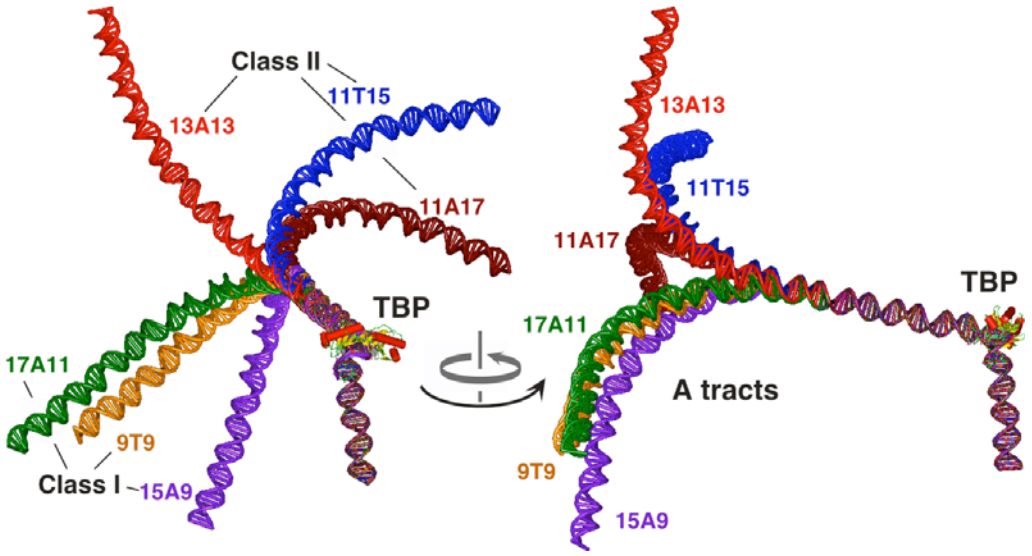

J. Kahn

Models for Free TATA-containing DNA

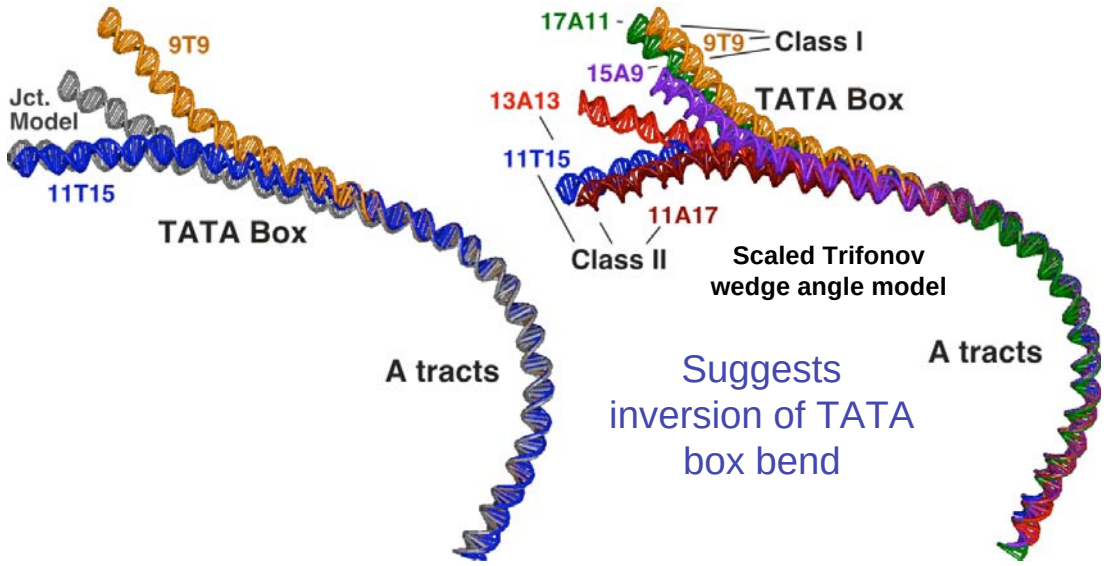

Suggests inversion of TATA box bend

J. Kahn

Cyclization Is Profoundly Affected by Shape

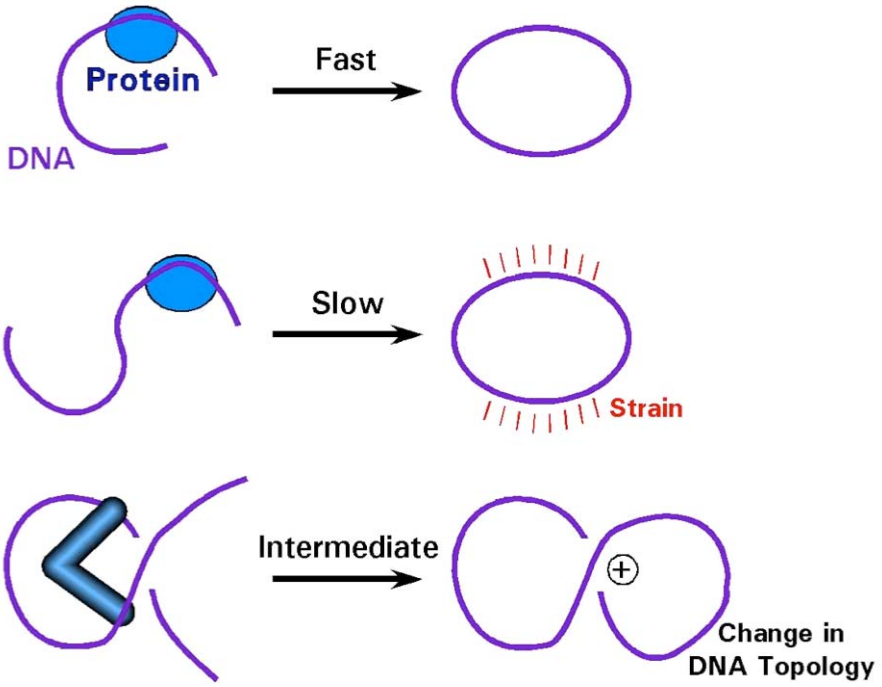

J. Kahn

Simultaneous Analysis of Equilibrium Constant and Cyclization Rate

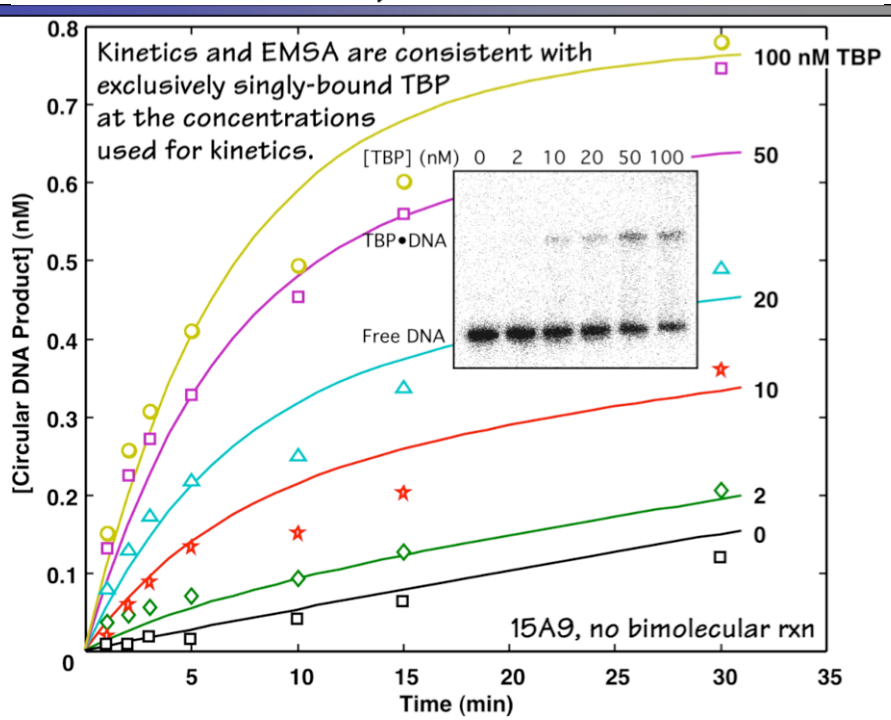

J. Kahn

Cyclization Kinetics for a Class I DNA (20A11) With and Without TBP

Simultaneous fitting of two kinetic experiments (Matlab):

- We can distinguish ±TBP reactions occuring in one tube
- The TBP-bound DNA cyclizes to give the -1 topoisomer
- J factors in this case are 110 nM for the TBP-induced -1 topoisomer and 8.1 nM for the free DNA 0 topoisomer.

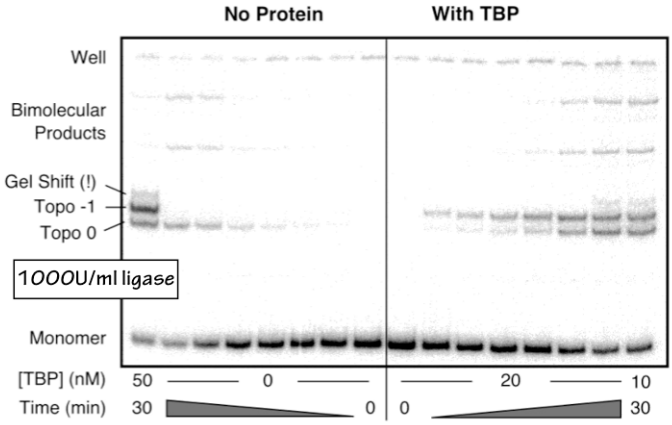

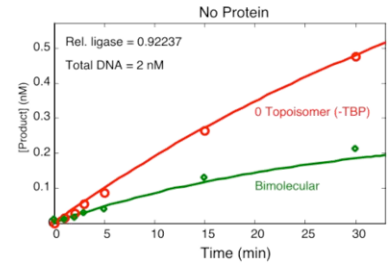

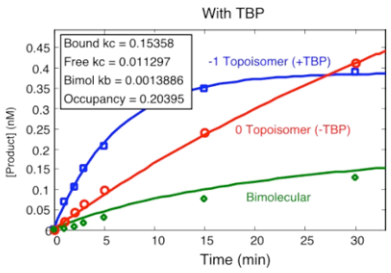

In-phase bending enhances cyclization. Topoisomers appear.

J. Kahn

TBP Represses Cyclization of the Out-of-phase (Class II) 8T15 Construct only Weakly, and the Cyclization of the Free DNA Is Surprisingly Rapid

- Rapid cyclization of free DNA suggests strong Bending or anisotropic flexibility of the TATA box; other data suggests it is anisotropic flexibility
- Difficult to measure true rate of TBP•DNA cyclization due to occupancy issues.

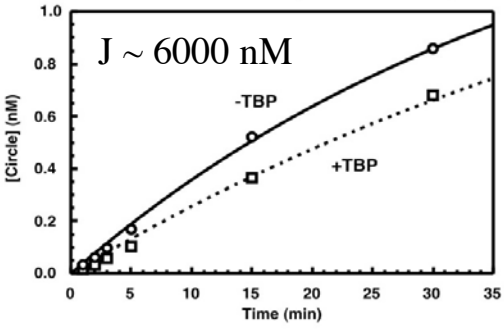

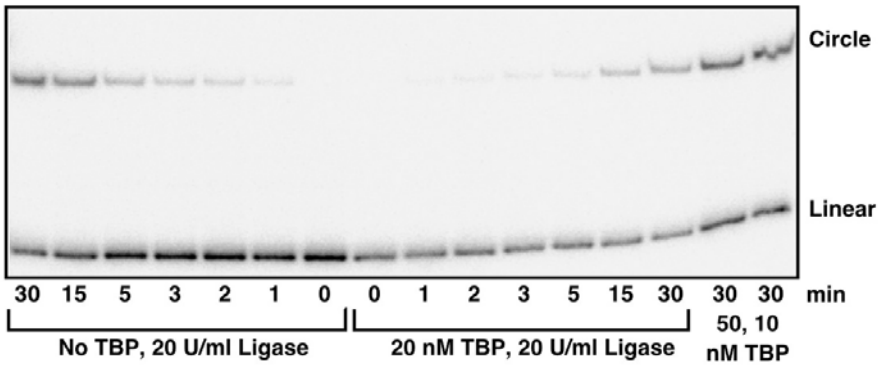

J. Kahn

DNA Topology

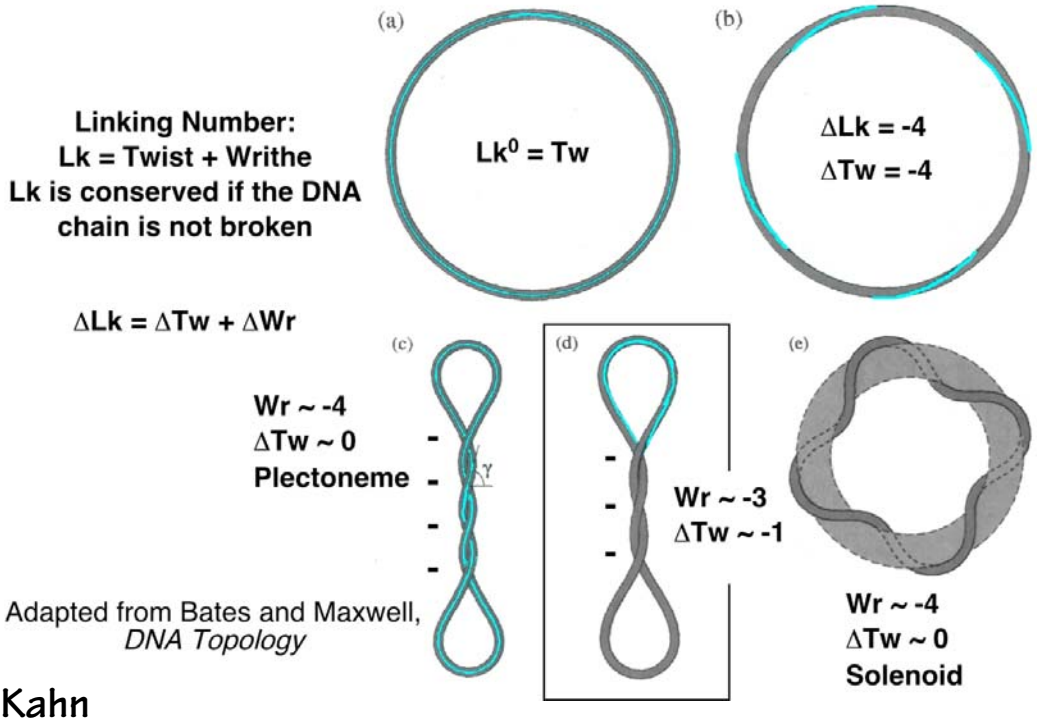

J. Kahn

Interconversion of Twist and Writhe

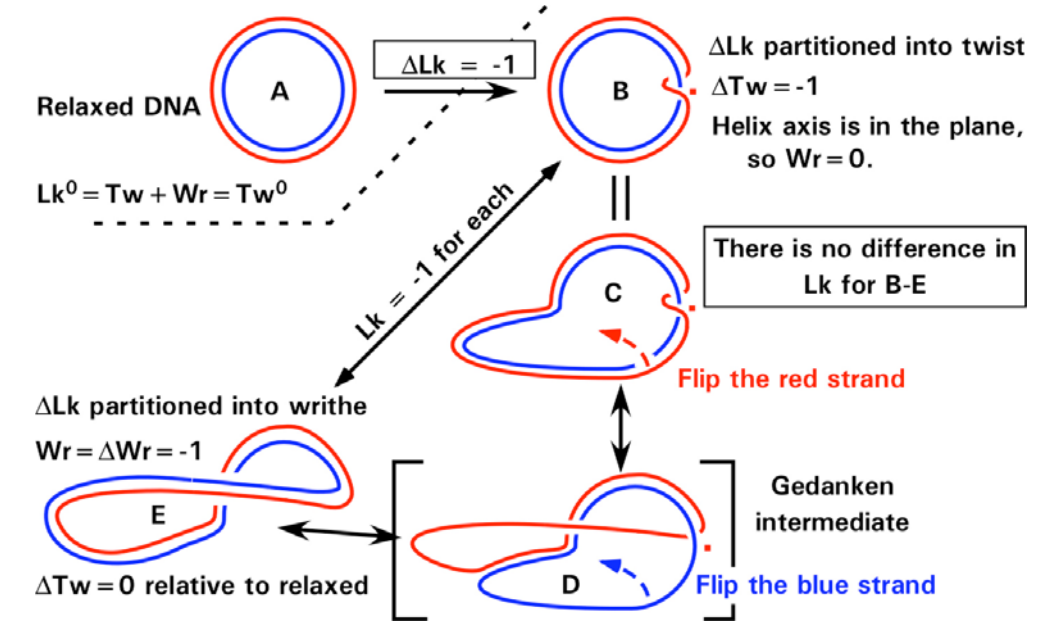

J. Kahn

Summary of Cyclization results for the TATA Box with and without TBP

Construct	Phasing	Total L / Turns §	147 bp 14.14	150 14.42	153 14.71	155 14.90	156 15.00	157 15.09	158 15.19	159 15.29	160 15.38	161 15.48	162 15.57	163 15.67
Class I: In-phase A-tract and TBP bends—TBP enhances cyclization														
(9)#T9	47 bp †	4.50	2.4*	2.3	13 (0) 1.7 (–)‡									
(9)T9+TBP	47	4.50	7700	470	140 (–)¶									
(15)A9	47	4.50			1.4		34			64				
(15)A9+TBP	47	4.50			6.9 (0) 5.3 (–)		710			28000				
(17)A11	49	4.69					54			14			7.8	
(17)A11+TBP	49	4.69					130			1200			150 (–)¶	
Class II: Out-of-phase A-tract and TBP bends—TBP represses cyclization except for unwinding effects														
(13)A13	51	4.88				6600			1200			1.1 (0) 1.3 (–)		
(13)A13+TBP	51	4.88				[3200]			[1200]			1.0 (0) 4.3 (–)		
(11)T15	53	5.07				5800			3500			8.5		
(11)T15+TBP	53	5.07				[4600]			[2200]			67 (0) 13 (+)		
(11)A17	55	5.26						6500			3700			1.6 (0) 1.2 (–)
(11)A17+TBP	55	5.26						[4000]			[2900]			840 (0)¶ 270 (–)¶

(n) indicates total length was varied by PCR by altering first linker length.
* All *J* factors (effective concentrations of aligned ends) are in nM.
† Distance from center of TATA box to center of first A tract: Half-integral turns indicates in-phase TBP-A tract bending.
§ Calculations assume B-DNA helical repeat = 10.45 bp/turn, A tracts 10.33 bp/turn, no allowance for TBP unwinding.
‡ Where (0), (–), or (+) are indicated, they accompany the *J* factors of the corresponding topoisomers.
¶ Estimate includes consideration of occupancy factor.

Bracketed values are upper limits; true values could be much lower due to site occupancy issues.
Results are reproducible to within a factor of 2.

Davis, Majee, and Kahn, JMB 1999.

Summary of Cyclization results for the TATA Box with and without TBP

Construct	Phasing	Total L / Turns §	147 bp 14.14	150 14.42	153 14.71	155 14.90	156 15.00	157 15.09	158 15.19	159 15.29	160 15.38	161 15.48	162 15.57	163 15.67
Class I: In-phase A-tract and TBP bends—TBP enhances cyclization														
(9)#T9	47 bp †	4.50	2.4*	2.3	13 (0) 1.7 (–)‡									
(9)T9+TBP	47	4.50	7700	470	140 (–)¶									
(15)A9	47	4.50			1.4		34			64				
(15)A9+TBP	47	4.50			6.9 (0) 5.3 (–)		710			28000				
(17)A11	49	4.69					54			14			7.8	
(17)A11+TBP	49	4.69					130			1200			150 (–)¶	
Class II: Out-of-phase A-tract and TBP bends—TBP represses cyclization except for unwinding effects														
(13)A13	51	4.88				6600			1200			1.1 (0) 1.3 (–)		
(13)A13+TBP	51	4.88				[3200]			[1200]			1.0 (0) 4.3 (–)		
(11)T15	53	5.07				5800			3500			8.5		
(11)T15+TBP	53	5.07				[4600]			[2200]			67 (0) 13 (+)		
(11)A17	55	5.26						6500			3700			1.6 (0) 1.2 (–)
(11)A17+TBP	55	5.26						[4000]			[2900]			840 (0)¶ 270 (–)¶

J factors are consistent with predicted bend magnitude and direction

(n) indicates total length was varied by PCR by altering first linker length.
* All *J* factors (effective concentrations of aligned ends) are in nM.
† Distance from center of TATA box to center of first A tract: Half-integral turns indicates in-phase TBP-A tract bending.
§ Calculations assume B-DNA helical repeat = 10.45 bp/turn, A tracts 10.33 bp/turn, no allowance for TBP unwinding.
‡ Where (0), (–), or (+) are indicated, they accompany the *J* factors of the corresponding topoisomers.
¶ Estimate includes consideration of occupancy factor.

Bracketed values are upper limits; true values could be much lower due to site occupancy issues.
Results are reproducible to within a factor of 2.

J. Kahn

Summary of Cyclization results for the TATA Box with and without TBP

Construct	Phasing	Total L / Turns §	147 bp / 14.14	150 / 14.42	153 / 14.71	155 / 14.90	156 / 15.00	157 / 15.09	158 / 15.19	159 / 15.29	160 / 15.38	161 / 15.48	162 / 15.57	163 / 15.67
Class I: In-phase A-tract and TBP bends—TBP enhances cyclization														
(9)#T9	47 bp †	4.50	2.4*	2.3	13 (0) 1.7 (–)‡									
(9)T9+TBP	47	4.50	7700	470	140 (–)¶									
(15)A9	47	4.50			1.4		34			64				
(15)A9+TBP	47	4.50			6.9 (0) 5.3 (–)		710			28000				
(17)A11	49	4.69					54			14			7.8	
(17)A11+TBP	49	4.69					130			1200			150 (–)¶	
Class II: Out-of-phase A-tract and TBP bends—TBP represses cyclization except for unwinding effects														
(13)A13	51	4.88					6600			1200		1.1 (0) 1.3 (–)		
(13)A13+TBP	51	4.88					[3200]			[1200]		1.0 (0) 4.3 (–)		
(11)T15	53	5.07					5800			3500		8.5		
(11)T15+TBP	53	5.07					[4600]			[2200]		67 (0) 13 (+)		
(11)A17	55	5.26						6500			3700			1.6 (0) 1.2 (–)
(11)A17+TBP	55	5.26						[4000]			[2900]			840 (0)¶ 270 (–)¶

Extremely efficient cyclization of TATA-containing DNA

(n) indicates total length was variable by ±1 bp to adjust for first linker length.
* All *J* factors (effective concentrations of aligned ends) are in nM.
† Distance from center of TATA box to center of first A tract: Half-integral turns indicates in-phase TBP-A tract bending.
§ Calculations assume B-DNA helical repeat = 10.45 bp/turn, A tracts 10.33 bp/turn, no allowance for TBP unwinding.
‡ Where (0), (–), or (+) are indicated, they accompany the *J* factors of the corresponding topoisomers.
¶ Estimate includes consideration of occupancy factor.

Bracketed values are upper limits; true values could be much lower due to site occupancy issues.
Results are reproducible to within a factor of 2.

J. Kahn

Summary of Cyclization results for the TATA Box with and without TBP

Construct	Phasing	Total L / Turns §	147 bp / 14.14	150 / 14.42	153 / 14.71	155 / 14.90	156 / 15.00	157 / 15.09	158 / 15.19	159 / 15.29	160 / 15.38	161 / 15.48	162 / 15.57	163 / 15.67
Class I: In-phase A-tract and TBP bends—TBP enhances cyclization														
(9)#T9	47 bp †	4.50	2.4*	2.3	13 (0) 1.7 (–)‡									
(9)T9+TBP	47	4.50	7700	470	140 (–)¶									
(15)A9	47	4.50			1.4		34			64				
(15)A9+TBP	47	4.50			6.9 (0) 5.3 (–)		710			28000				
(17)A11	49	4.69					54			14			7.8	
(17)A11+TBP	49	4.69					130			1200			150 (–)¶	
Class II: Out-of-phase A-tract and TBP bends—TBP represses cyclization except for unwinding effects														
(13)A13	51	4.88					6600			1200		1.1 (0) 1.3 (–)		
(13)A13+TBP	51	4.88					[3200]			[1200]		1.0 (0) 4.3 (–)		
(11)T15	53	5.07					5800			3500		8.5		
(11)T15+TBP	53	5.07					[4600]			[2200]		67 (0) 13 (+)		
(11)A17	55	5.26						6500			3700			1.6 (0) 1.2 (–)
(11)A17+TBP	55	5.26						[4000]			[2900]			840 (0)¶ 270 (–)¶

TBP-induced topoisomers appear at ~n+0.6 helical turns: ΔLk ~ −0.3

Extremely efficient cyclization of TATA-containing DNA

(n) indicates total length was variable by ±1 bp to adjust for first linker length.
* All *J* factors (effective concentrations of aligned ends) are in nM.
† Distance from center of TATA box to center of first A tract: Half-integral turns indicates in-phase TBP-A tract bending.
§ Calculations assume B-DNA helical repeat = 10.45 bp/turn, A tracts 10.33 bp/turn, no allowance for TBP unwinding.
‡ Where (0), (–), or (+) are indicated, they accompany the *J* factors of the corresponding topoisomers.
¶ Estimate includes consideration of occupancy factor.

Bracketed values are upper limits; true values could be much lower due to site occupancy issues.
Results are reproducible to within a factor of 2.

J. Kahn

Summary of Cyclization results for the TACA Box, without TBP

Construct	Phasing	Total L / Turns §	147 bp 14.14	150 14.42	153 14.71	155 14.90	156 15.00	157 15.09	158 15.19	159 15.29	160 15.38	161 15.48	162 15.57	163 15.67
Class I: Out-of-phase A-tract and TACA box bends														
(9)#T9	47 bp †	4.50	0.76	1.1	0.71									
(15)A9	47	4.50			1.8		10			2.8				
(17)A11	49	4.69					16			3.2			0.42	
Class II: In-phase A-tract and TACA box bends														
(13)A13	51	4.88				410			54			0.7 (0) 0.2 (–)		
(11)T15	53	5.07				640			250			1.9		
(11)A17	55	5.26						320			29			0.4 (0) 0.5 (–)

All of the *J* factors are lower for the TACA box than for the corresponding TATA box:
TACA looks more like a plain A tract.
➔ Suggests decreased bending/flexibility.

Flexibility of the TATA box is readily disrupted by a single-base change.
➔ Suggests TATA box deformability is essential to recognition by TBP.

J. Kahn

Comparisons with FRET and other literature results suggest roles for TATA box flexibility

FRET: Parkhurst, Richards, Brenowitz & Parkhurst(1999). *JMB* **289**, 1327-1341.
Variant Structures: Patikoglou, Kim, Sun, Yang, Kodadek, & Burley (1999). *Genes Dev.* **13**, 3217-3230.

FRET: High ΔH, Slow, Fast

$$\text{TBP + DNA} \rightleftharpoons \text{TBP·DNA I1 (Bent)} \rightleftharpoons \text{I2 (Bent)} \rightleftharpoons \text{Final}$$

Interpretation:

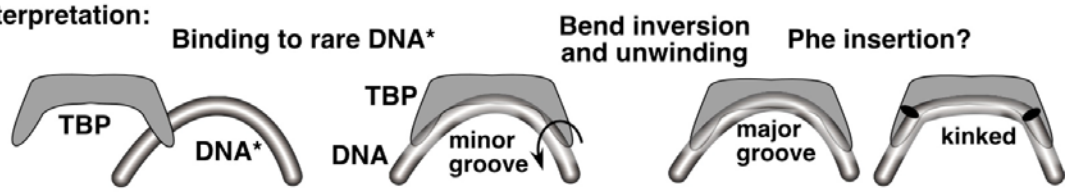

TBP binding to DNA is slow -- Why?
Requires binding to rare pre-bent state.
Binding to some TATA variants is poor, though final complexes all look similar -- Why?
DNA is not readily deformable: it is the reactant's free energy that is sensitive to mutation, not the product's.
Is there a clear function for Phe intercalation?
Compensates for topological change induced by unwinding: TBP is a "facultative supercoiler."

J. Kahn

Further testing of TATA-TACA flexibility

- Identified intrinsic bendability correlates with the binding affinity of TBP but not final structure.
- Ligation ladders do not suggest unusual bending, suggests anisotropic flexibility.
- Theoretical work (Manning, Maddocks) using rod mechanics focuses on double-well hinge to explain results.
- Possible relationship to Widom results on hyperflexible DNA.
- Predict that cryo-EM (Bednar, Dubochet, Amzallag) on minicircles vs. linear should show a strong induced kink at TATA. May not be panning out…
- Advanced NMR and X-ray by others, please.

J. Kahn

What about the supercoiling?

- In plasmid relaxation experiments (Roger Kornberg), no ΔLk was observed.
- X-ray structures showed 100° untwisting, compensated by positive writhe (~0.25).
- Is there a simple structural change that can explain our observations?

J. Kahn

DNA Deformation Induced by TBP

Intercalating phenylalanines are responsible for out-of-plane bending, and there is substantial bending by roll across the top of the saddle

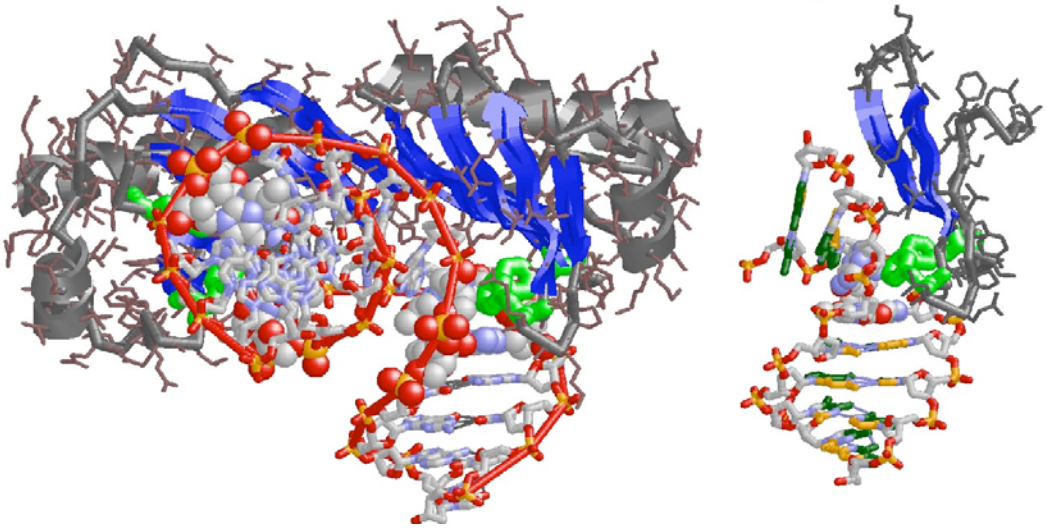

J. Kahn

Speculative "Stirrup Retraction" Model for Flattening of the TBP•DNA Complex

Remove roll kinks at stirrups. No other changes

Roll/tilt/twist angles from hTBP-DNA

- Bend magnitude is essentially unchanged!
- Induced bend is rotated slightly relative to neighboring DNA
- Slight extension of the molecule

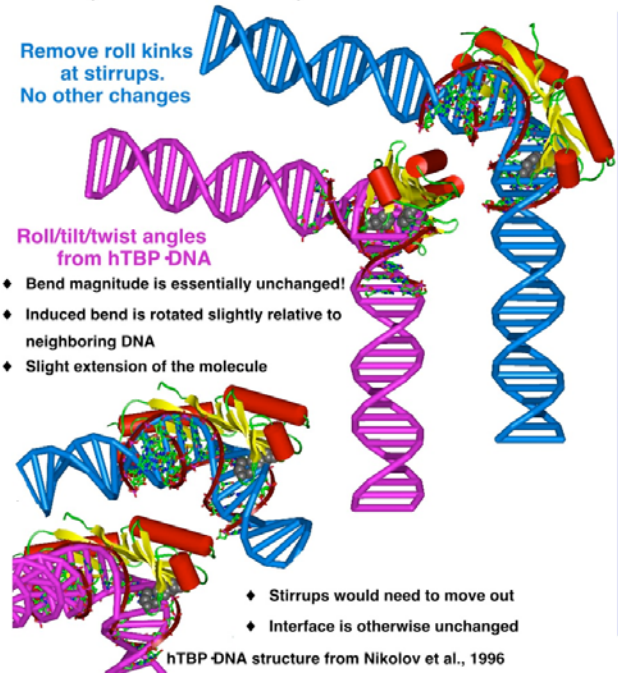

- Stirrups would need to move out
- Interface is otherwise unchanged

hTBP-DNA structure from Nikolov et al., 1996

The Consequences of Kink Removal Are More Topological than Geometric

- DNA is flattened: No more writhe!
- Twist is unchanged inside site
- Requires overtwisting outside—that's where the lost positive ΔWr goes

J. Kahn

Model for Minicircle Flattening

Modest Structural Change Can Decrease Writhe Substantially. TBP May Be Able to Act as a "Supercoil Shock Absorber"

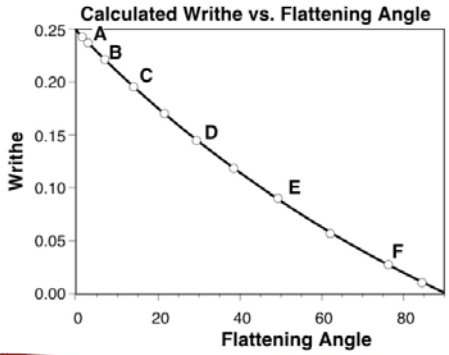

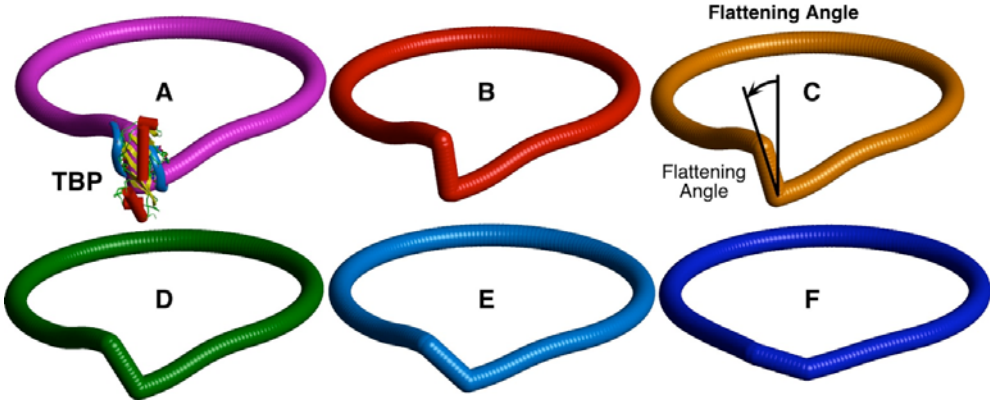

J. Kahn

TBP Malleability in Different Complexes

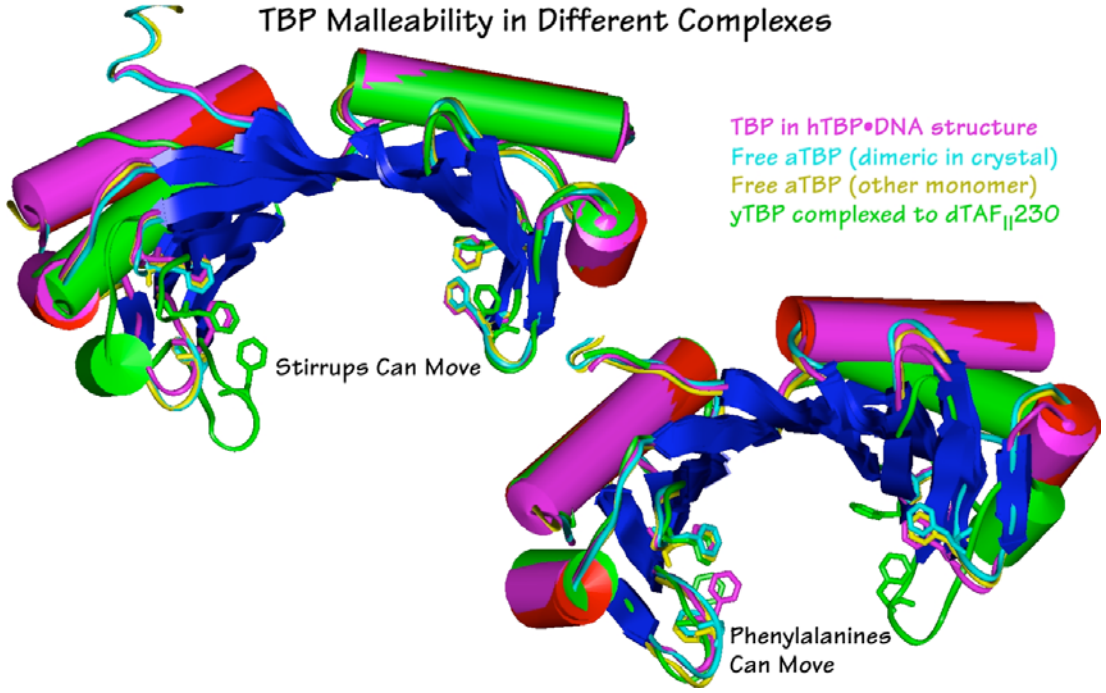

J. Kahn

Why Should TBP Flatten?

- Flattening induces longer contour length and eliminates out-of-plane bending.
- In a minicircle environment, this will allow an increased radius of curvature and decreased writhe in the remainder of the molecule.
- The driving force for flattening is thus the relief of bending strain in the remainder of the minicircle.
- Why we care: model for strained DNA in vivo?

J. Kahn

Testing Strain-induced Flattening Mechanism

- The effect should decrease as length increases: Measure DNA length-dependence of induced supercoiling.
- TBP should bind better to appropriate negatively supercoiled minicircles than to anything else. Footprint and EMSA to measure stability and kinetics.
- Reality check using Monte Carlo simulations of DNA cyclization.
- TBP mutants that lack Phe stirrups should be "obligate supercoilers." Some TBP-like factors may be natural examples.

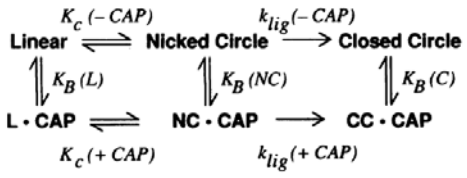

$$\frac{J(+CAP)}{J(-CAP)} \cong \frac{K_c(+CAP)}{K_c(-CAP)} = \frac{K_B(NC)}{K_B(L)} = \frac{K_B(C)}{K_B(L)}$$

J. Kahn

DNA Length Dependence of TBP/TFIID-induced Topological Changes

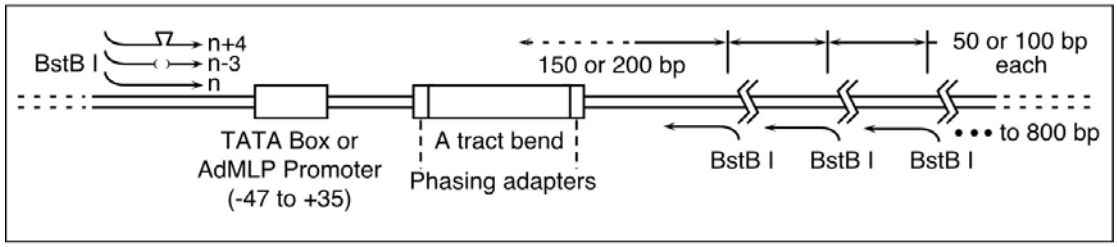

Length variation probes for size- and flexibility-dependence of observed unwinding.

- The topological coupling model predicts that as the DNA length increases the driving force for minicircle flattening decreases, as the DNA is more flexible.
- Thus TBP•DNA should revert to the presumed ground state as DNA size increases.
- The use of "poised" DNA lengths maximizes the sensitivity to changes in torsion,
- A family of molecules with base lengths 150, 200, 250, 300, 350...800 bp are synthesized by PCR using the primers shown. That PCR primer from the set of three at the left is chosen which provides two (or more) topoisomers upon cyclization.

J. Kahn

DNA Length Dependence of Topological Change

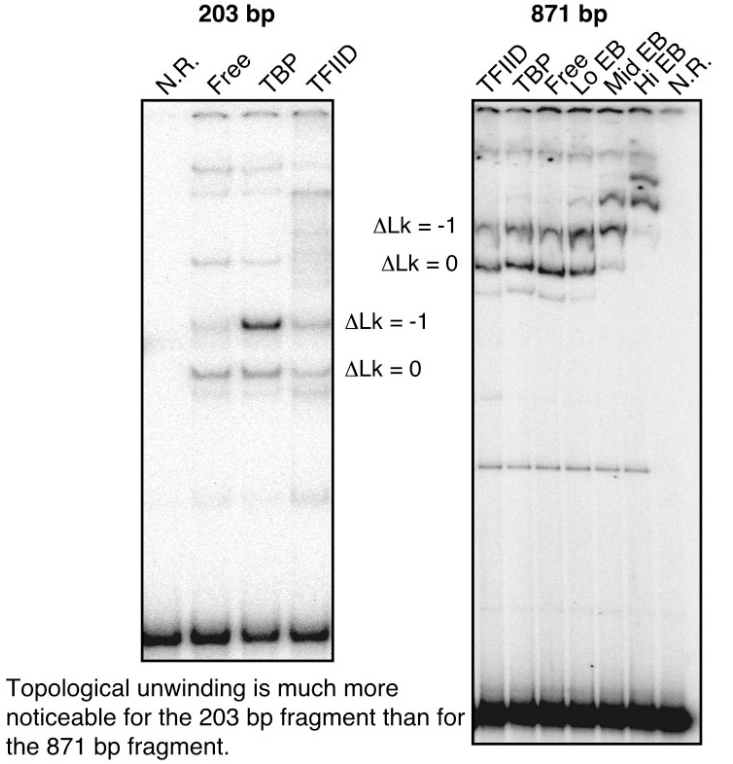

Topological unwinding is much more noticeable for the 203 bp fragment than for the 871 bp fragment.

J. Kahn

Effect of TBP/TFIID on Topology Decreases Rapidly with Increasing DNA Length

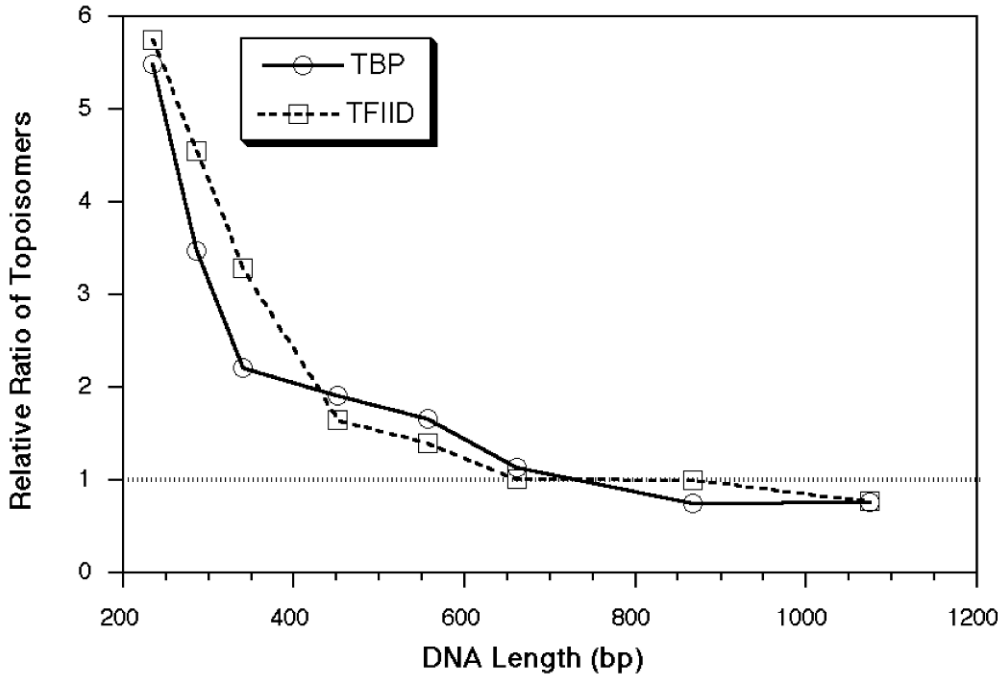

J. Kahn

HO• Footprinting and EMSA of Supercoiled Minicircles

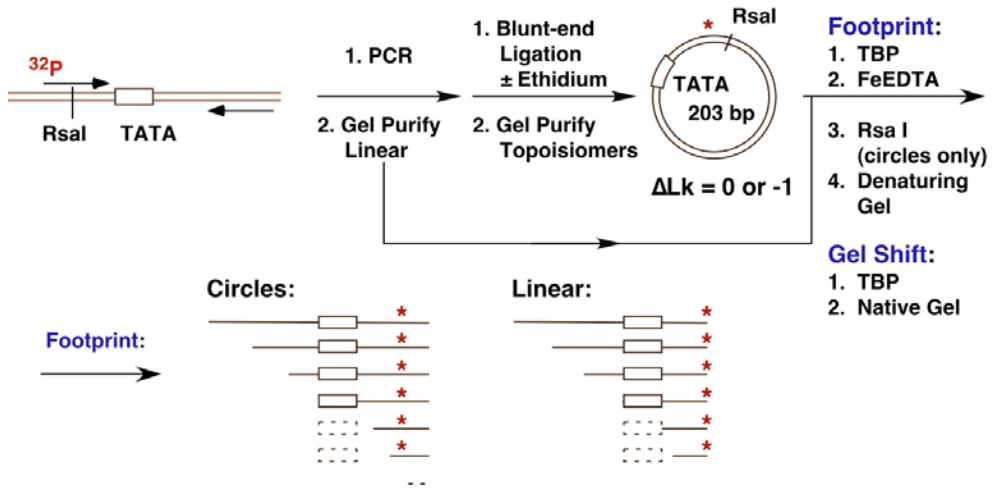

J. Kahn

Gel Mobility Shift of -1 Topoisomer and Linear DNA with TBP

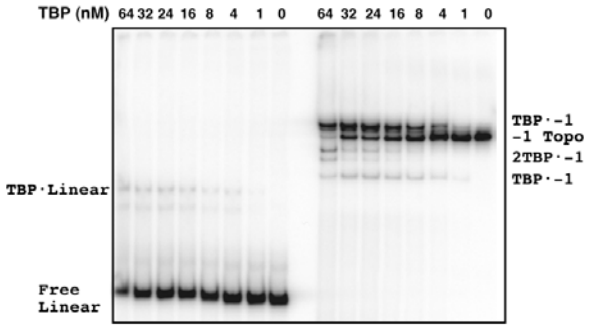

Circle is much more stable in the gel, shows modestly increased binding affinity

Gel Mobility Shift of O Topoisomer and Linear DNA

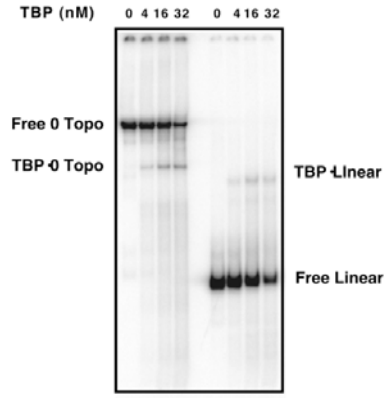

Gels suggest global conformational changes

- TBP affects R_g of circle much less than that of linear.
- Acceleration due to induced writhe.
- Difficult to measure binding affinity with any confidence: We (and others) do not observe saturation on linear DNA, suggesting kinetic instability. Circles are stable.

J. Kahn

Hydroxyl Radical Footprinting of -1 Topoisomer

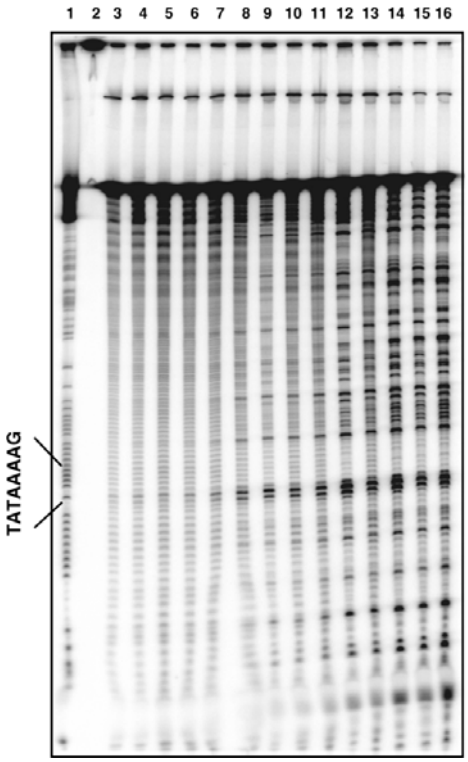

Binding curve for TBP with the -1 Topoisomer

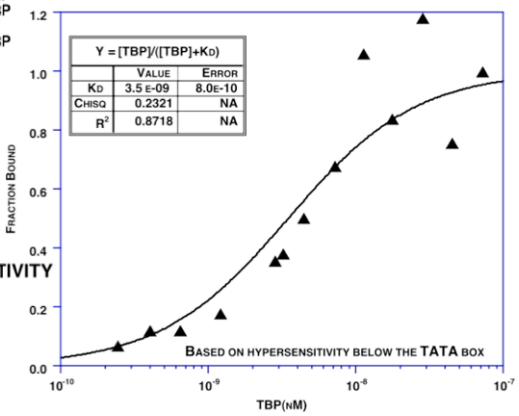

J. Kahn

Monte Carlo Simulation

- Levene, Crothers, Drak. Also Hagerman.
- Specify models for intrinsic curvature, induced bending, and bending and torsional flexibility. Can consider arbitrary potentials.
- Build ensemble of DNA half-chains using rotation matrices to generate coordinates for each base pair from the previous one.
- Filter joined ensembles for end-to-end contact, axial and torsional alignment.
- Calculate *J* factors and the Twist, Writhe, and Link of cyclized chains (observe only integral Lk).
- Newer methods for bent DNA:
  - Manning, Maddocks, Kahn, 1996 use rod mechanics to calculate equilibrium shapes.
  - Zhang and Crothers, 2003 use iterative annealing to obtain equilibrium and then harmonic expansion to consider entropy.

J. Kahn

Monte Carlo Simulations of DNA Topology vs. Length, ± TBP Flattening

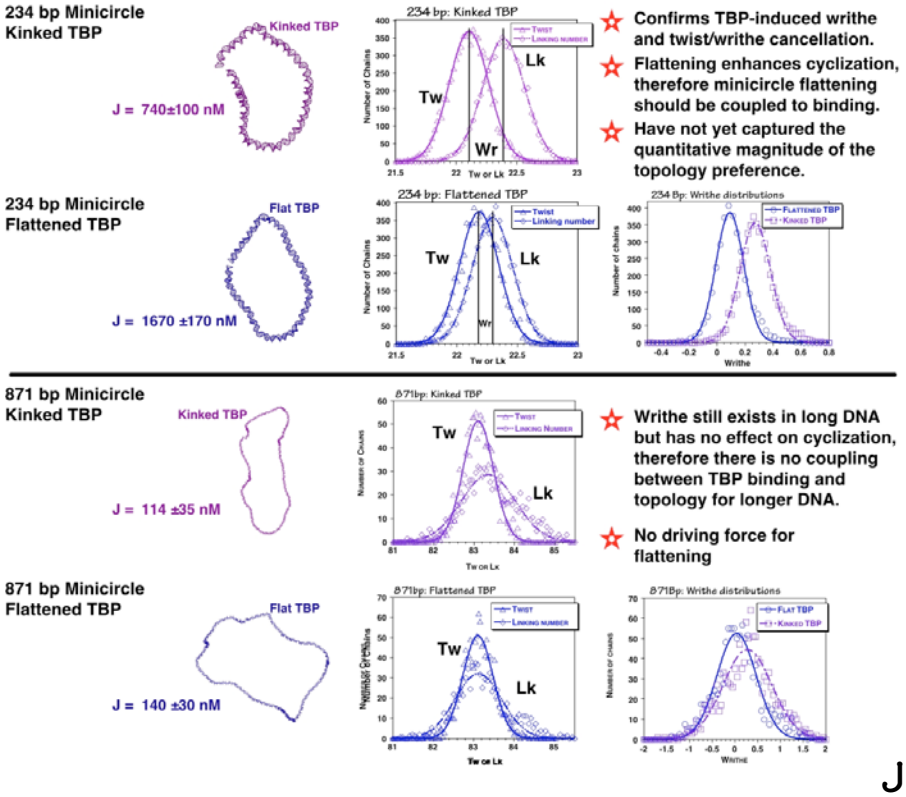

J. Kahn

Why is this worth our effort?

- Unusual (unique?) example of a strain-responsive conformation for a protein-DNA complex
- Biological relevance to transcription on constrained/supercoiled DNA templates.
- Superhelical strain can be dynamic as well as static: possible broad importance.
- Where does supercoiling appear…?

J. Kahn

Chromatin Structure: Nucleosome and 30 nm fiber

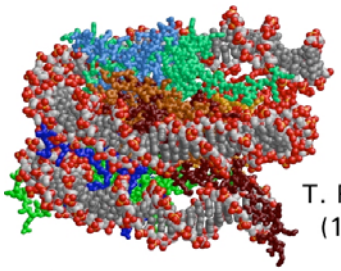

T. Richmond
(1aoi.pdb)

1.65 Turns of Left-Handed Superhelix
But ΔLk ~ −1/Nucleosome

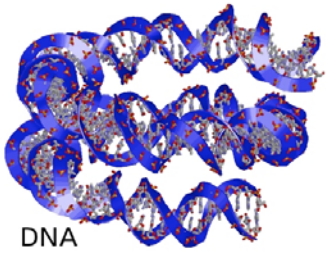

DNA

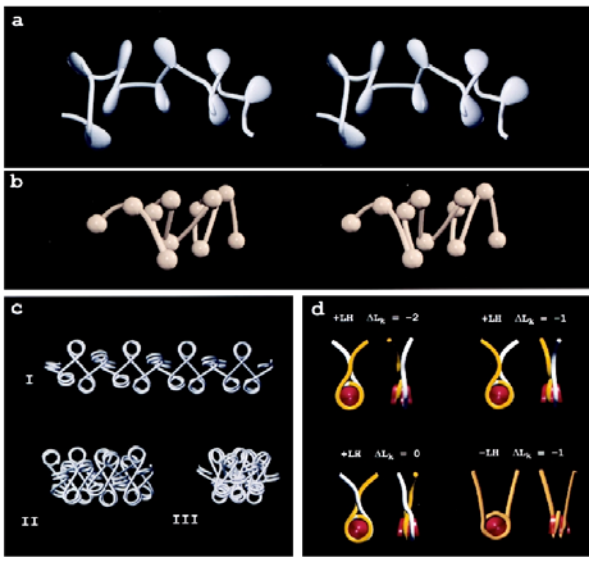

Bednar et al., 1998, PNAS

J. Kahn

Models for Chromatin Remodeling by ATPase Motor Proteins

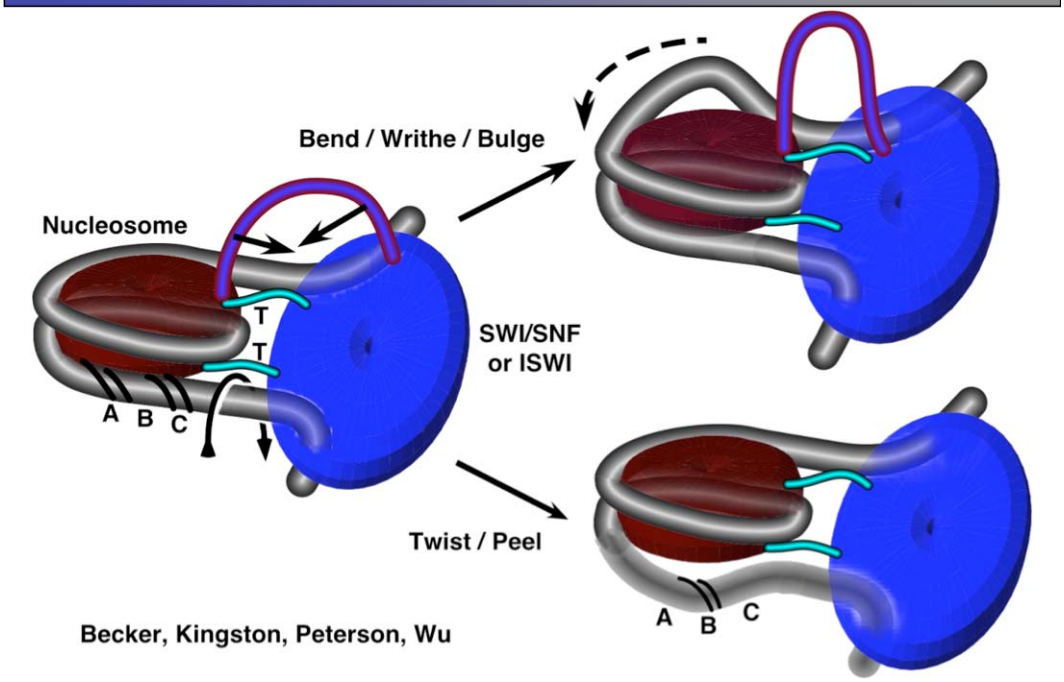

J. Kahn

Proposed Coupling of Supercoiling Changes with TBP Binding in a Constrained Chromatin Context

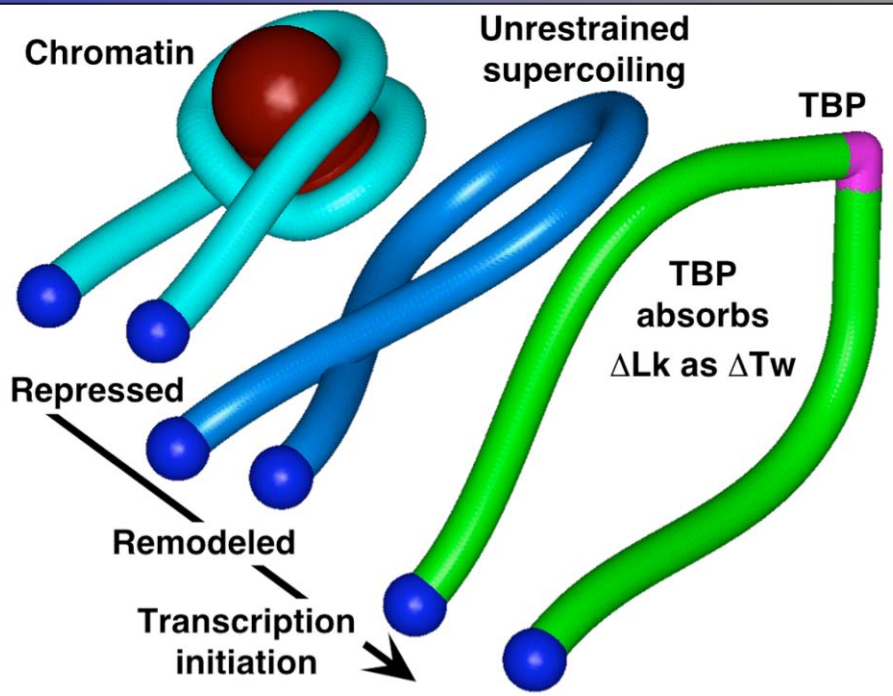

Kahn, Biochemistry 2002

J. Kahn

Testing Supercoiling-Binding -Remodeling Connections

- Test remodeling of reconstituted nucleosomes in minicircles and the effect on remote TBP
- In vivo analysis of rate of TBP binding and/or transcription initiation after remodeling? ChIP, Re-ChIP
- Analyze Phe stirrup mutants and TLF's lacking Phe stirrups

J. Kahn

Communication Between Nucleosomes and TBP?

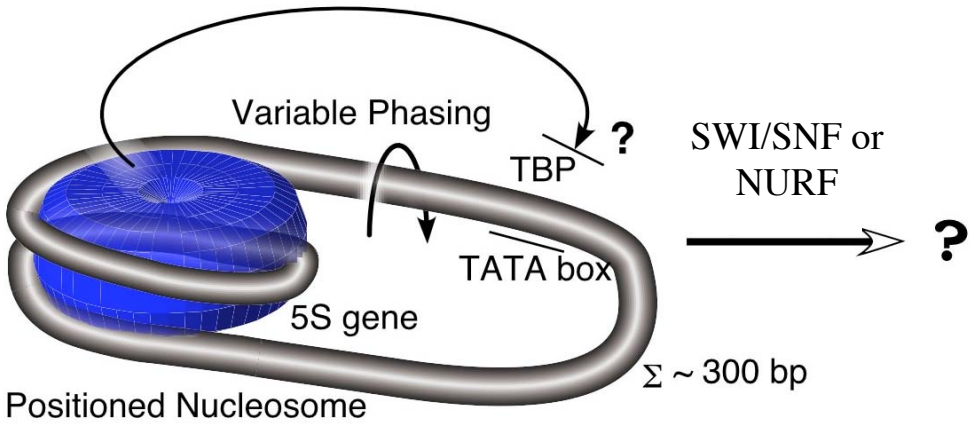

J. Kahn

TBP-like factors (Moras, Tora)

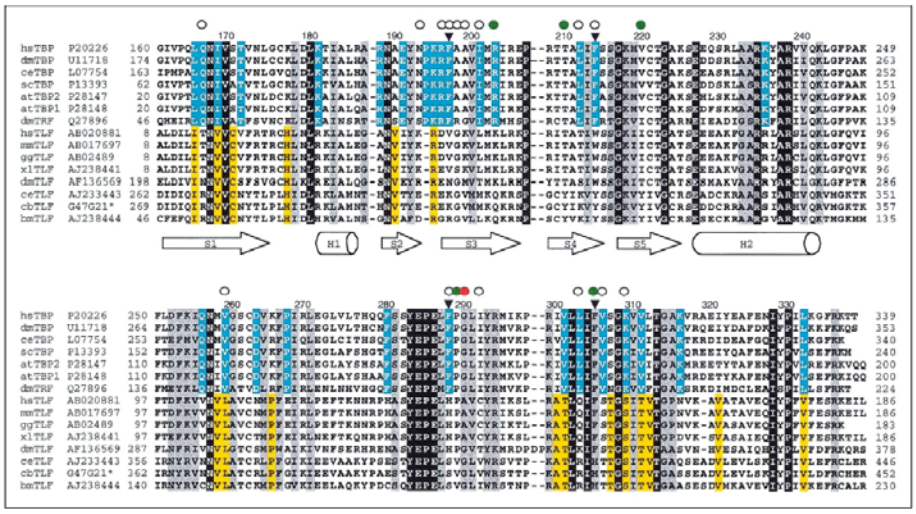

Figure 1

Sequence alignment of the conserved N- and C-terminal repeats of the core domains of TATA-binding proteins (TBPs) with the corresponding domains of the newly identified TBP-like factors (TLFs) and the *Drosophila* TBP-related factor (TRF). The amino acid one-letter code is used. Numbers indicate the starting and the ending amino acid positions of the N-terminal (top) and C-terminal (bottom) repeats. The positions of the α helices (H) and the β strands (S) for both repeats are also labelled. Residues conserved among TBPs, TLFs and the TRF have a black background; residues with the same physicochemical properties in all factors are on a grey tint; TBP- and TRF-specific residues are blue; TLF-specific residues are yellow. Coloured circles indicate key amino acids also depicted in Figure 3. Arrowheads indicate the two phenylalanine pairs conserved in TBPs. Accession numbers for each sequence are indicated. Abbreviations: at, *Arabidopsis thaliana*; bm, *Brugia malayi*; cb, *Caenorhabditis briggsae*; ce, *Caenorhabditis elegans*; dm, *Drosophila melanogaster*; gg, *Gallus gallus*; hs, *Homo sapiens*; mm, *Mus musculus*; sc, *Saccharomyces cerevisiae*; xl, *Xenopus laevis*.

J. Kahn

TBP-TATA Summary

- The TATA box DNA is remarkably, anisotropically, cooperatively flexible, and this may be important to the mechanism of TBP binding and sequence selectivity.
- TBP induces ΔLk of about -0.3 in small minicircles, perhaps due to “stirrup retraction.” Removal of positive writhe contribution allows untwisting to manifest in the linking number. This leads to improved binding to negatively supercoiled minicircles.
- Length dependence of supercoiling is consistent with unusual strain-induced plasticity of the TBP-DNA complex.
- Suggests possible role for this effect as a “supercoil shock absorber,” coupling chromatin remodeling to time-dependent activation of TBP binding.

J. Kahn

Acknowledgments – TBP

- Dr. Natalie A. Davis
- Dr. Sangita Sen Majee
- Jung Byun
- Mein Samala
- Chris McPhee

- Dr. Michael Brenowitz (Albert Einstein)
- Dr. Stephen Burley (Rockefeller, then)
- Dr. Mike Carey (UCLA)
- Dr. Alan Wolffe
- Drs. Rob Manning (Haverford) and John Maddocks (EPFL)
- Drs. Jacques Dubochet (Lausanne) and Jan Bednar (Grenoble)

J. Kahn

The *lac* Operon: DNA Looping Paradigm

Tetrameric Lac repressor protein binds two DNA sites (operators). The secondary operators increase the local concentration of repressor in the neighborhood of the primary operator via DNA looping. This is essential for efficient repression of gene expression.

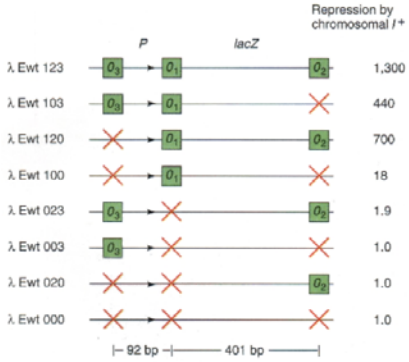

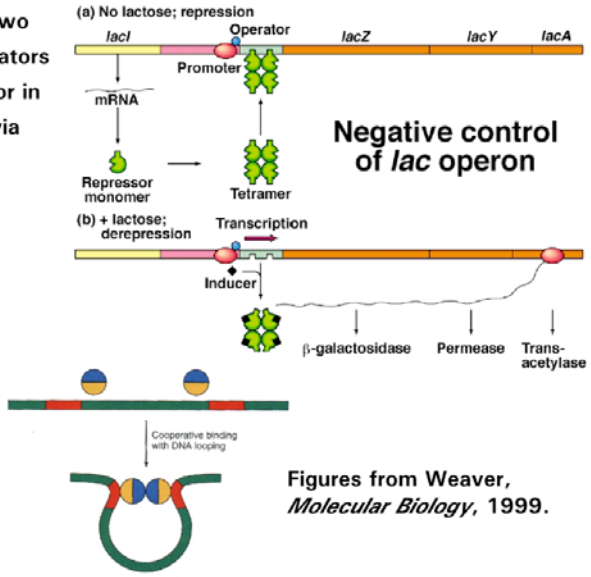

Figures from Weaver, *Molecular Biology*, 1999.

J. Kahn

"Lewis Model" for the LacI-DNA Loop

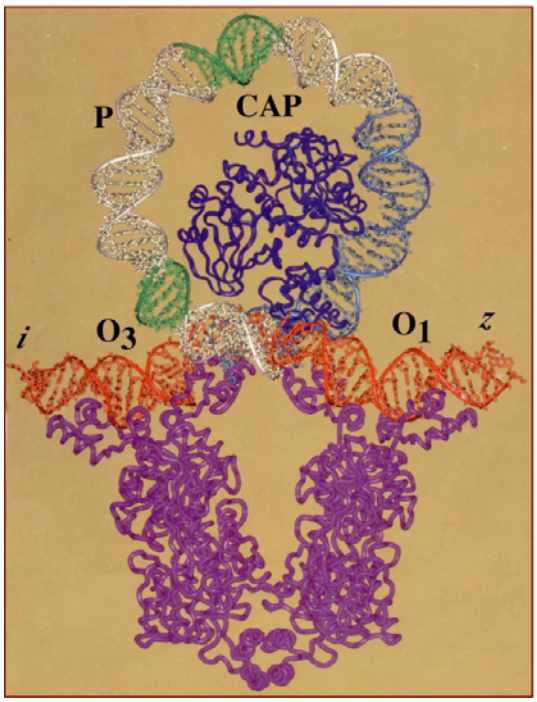

Lewis, M. *et al.* (1996). "Crystal Structure of the Lactose Operon Repressor and Its Complexes with DNA and Inducer." *Science* 271, 1247-1254. (Cover)

Issues:

- Discontinuous DNA
- CAP and Lac binding sites on opposite faces
- Positive supercoil

J. Kahn

Testing Models for Lac Repressor Looping

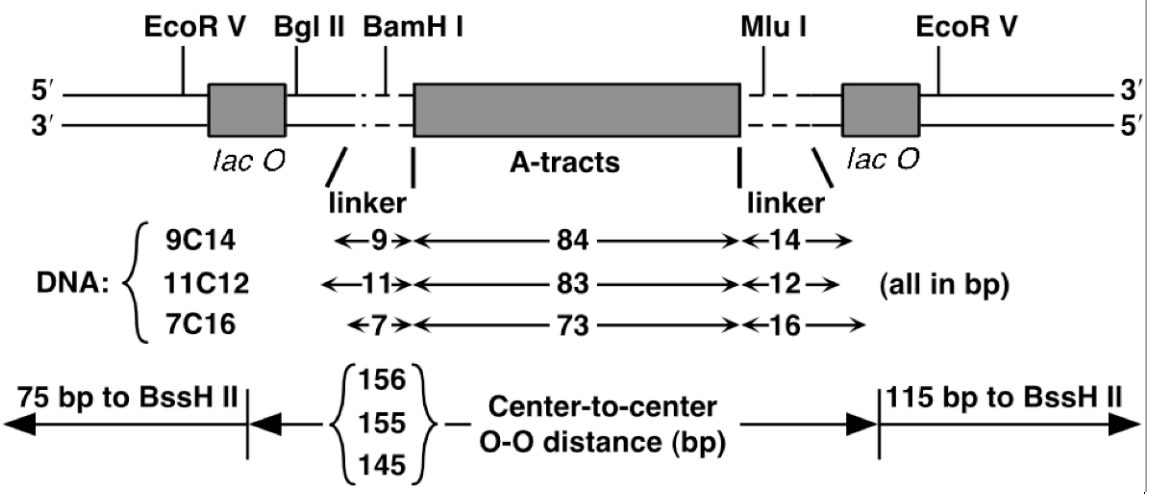

What do these DNA constructs look like?

J. Kahn

Constructs Designed to Stabilize Different Plausible Loops

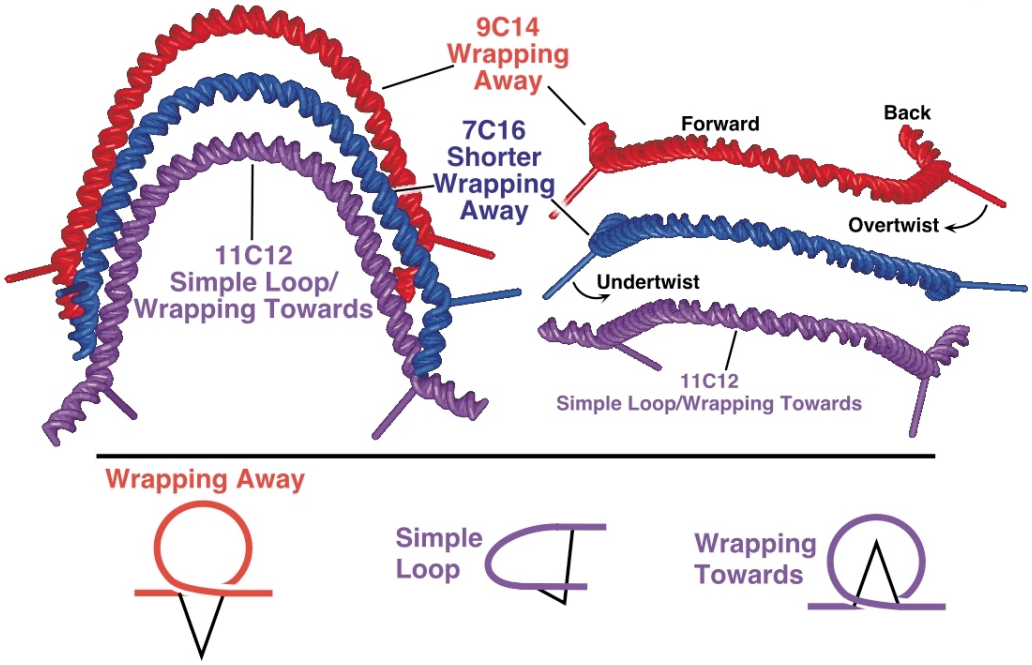

- *The DNA shape that most resembles that preferred by Lac repressor should form the most stable loop.*

J. Kahn

DNA Loop Equilibria

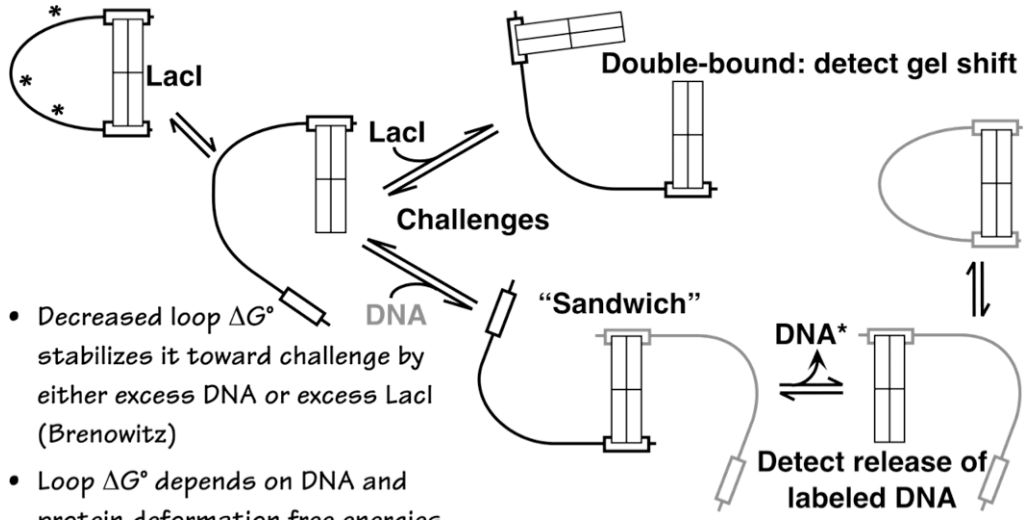

- Decreased loop ΔG° stabilizes it toward challenge by either excess DNA or excess LacI (Brenowitz)
- Loop ΔG° depends on DNA and protein deformation free energies

J. Kahn

Stability of Designed Loop Constructs to Protein Challenge: Loops are stable, have different gel mobilities

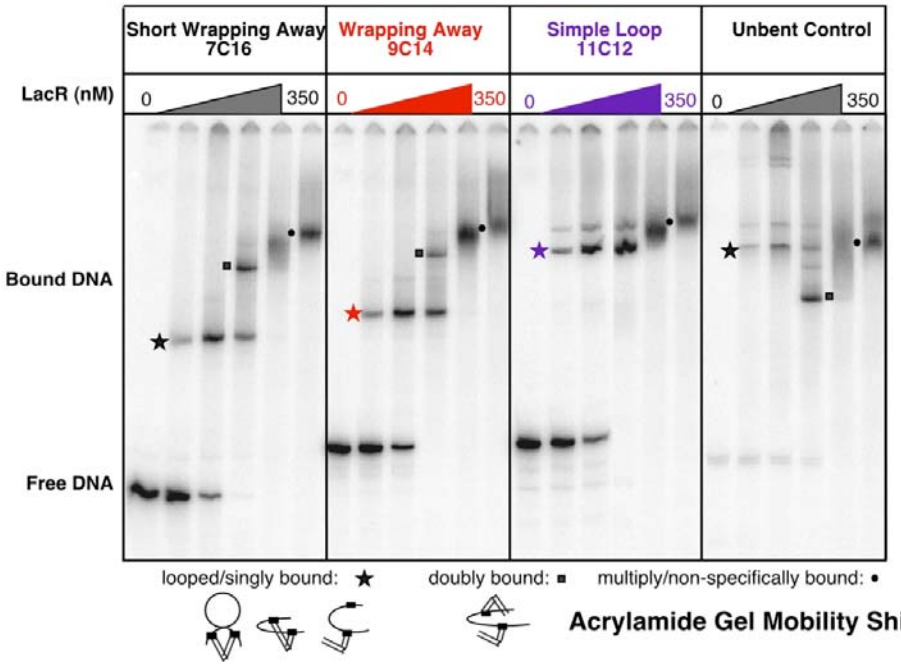

J. Kahn

Stability of LacI-mediated Loops to Competitor DNA Challenge: Both Designed Loops Are Kinetically Hyperstable.

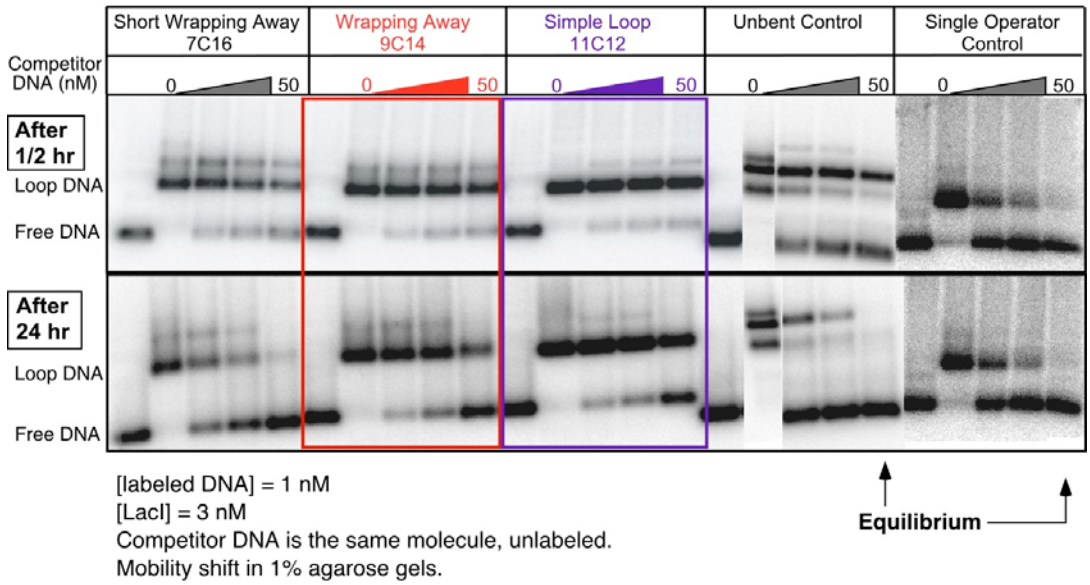

[labeled DNA] = 1 nM
[LacI] = 3 nM
Competitor DNA is the same molecule, unlabeled.
Mobility shift in 1% agarose gels.

J. Kahn

EMSA Competition results

- Confirms formation of hyperstable loops
- Surprisingly, both geometric designs worked.
- What shapes are formed?

J. Kahn

Cyclization Is Profoundly Affected by Shape

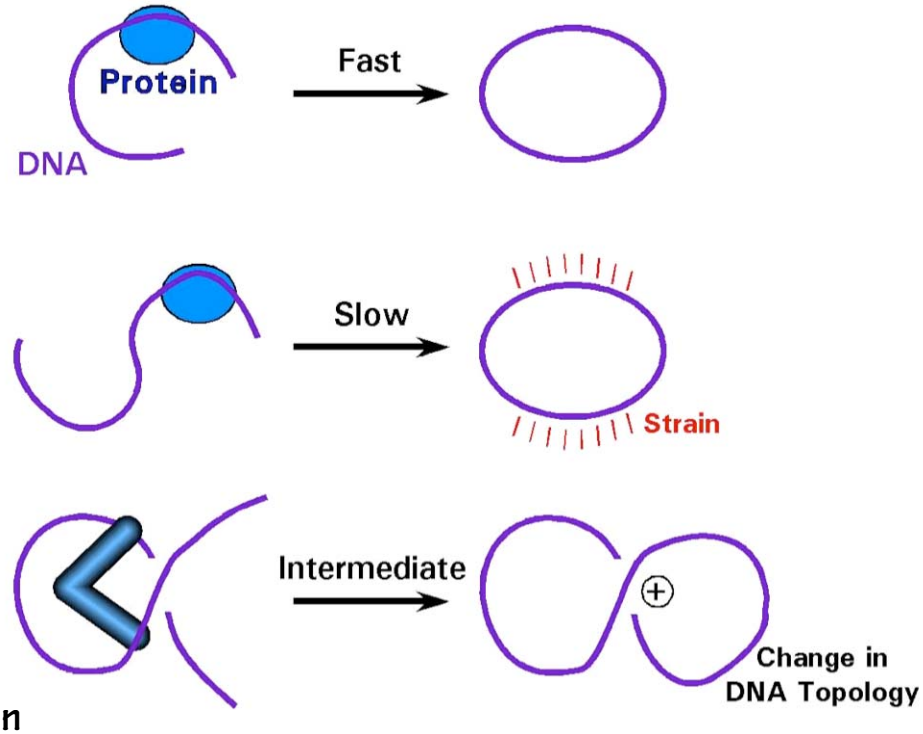

J. Kahn

Cyclization Kinetics of Extended Constructs

Extend Constructs from EcoR V to BssH II for Cyclization of ~340 bp Fragments

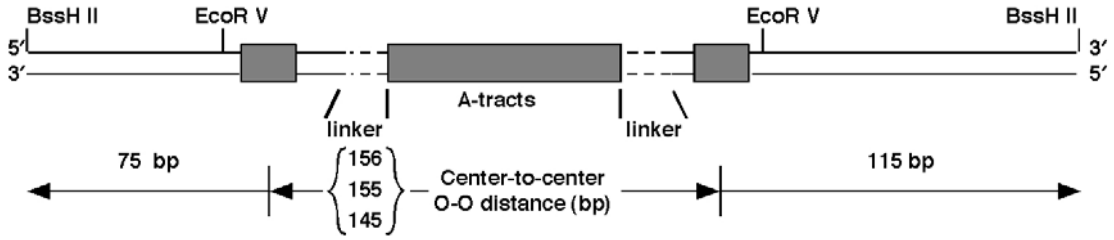

- **Measure T4 DNA ligase mediated cyclization kinetics with and without LacI**
- **Focus on changes in the topology of circular products**
- ***J* Factors (effective concentration of one DNA end in the neighborhood of the other) also measured**

J. Kahn

Ligation Kinetics of Extended LacI Looping Constructs

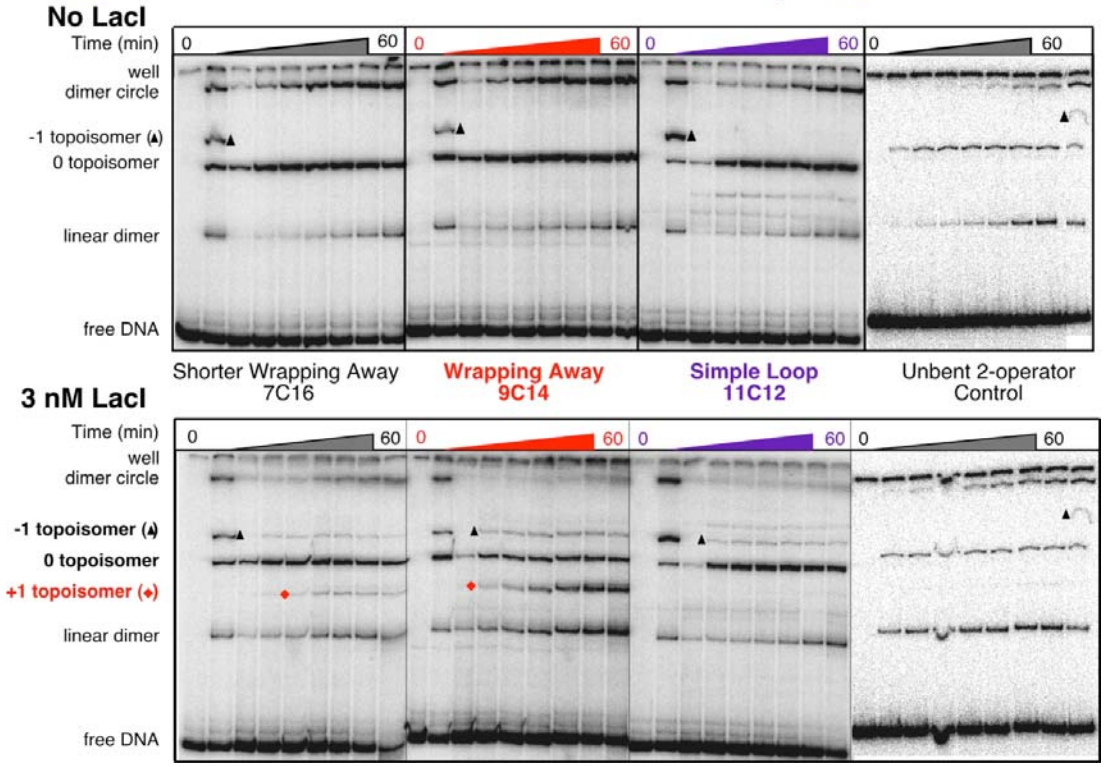

Conclusions from Biochemical Experiments

- Successful design of hyperstable loops.
- Open form 11C12 (purple) is the most stable, geometry appears to mimic unbiased loop. Forms relaxed circle.
- Ring closure experiments show that the less stable wrapping away 9C14 (red) forms relaxed circle and positive supercoil. Kinetics suggest a mixture of structures.
- **MODEL?**

- Mehta and Kahn, JMB 1999

J. Kahn

Proposed Loop Geometries

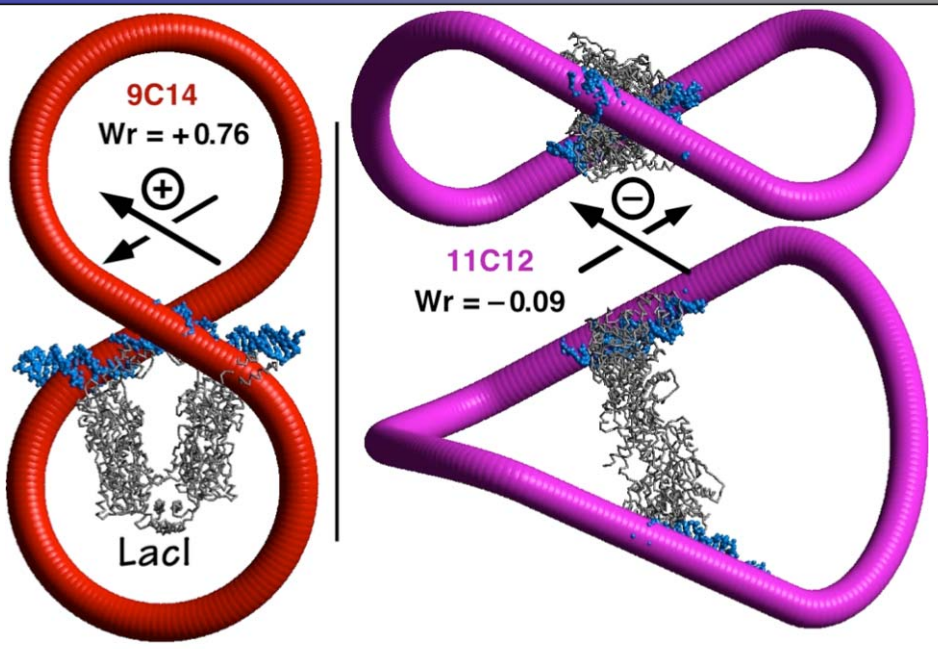

Can be forced to form: balance of stresses

More stable, proposed mimic for natural loop

J. Kahn

Crystal Structure of LacI•DNA (Lewis et al., 1996)

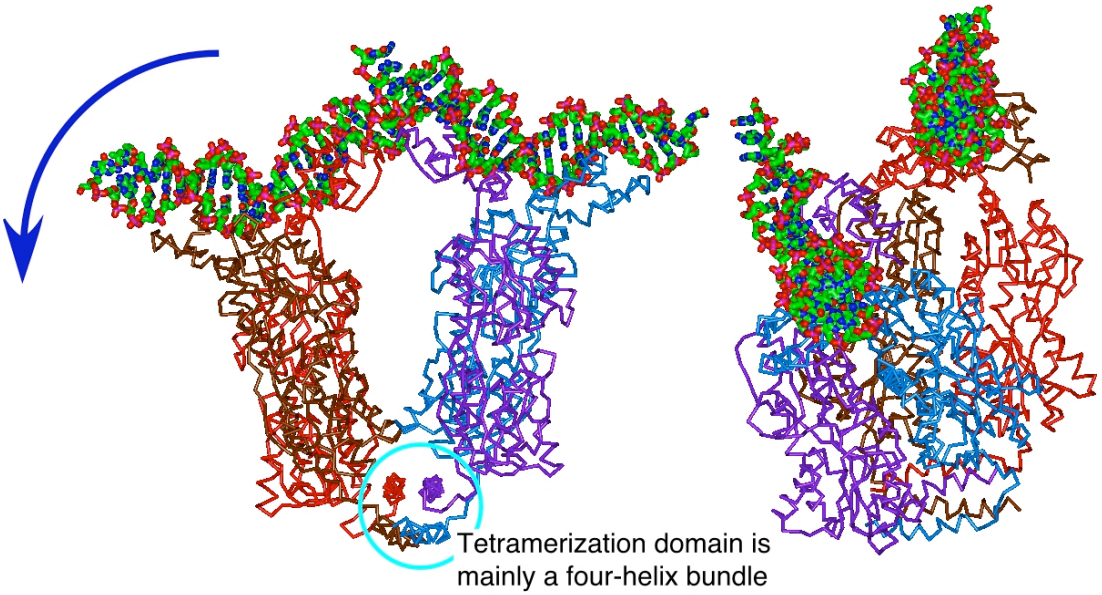

Opening model cf. Friedman, Fischmann and Steitz, 1995

J. Kahn

Plausible "Open Form" of LacI Tetramer•DNA

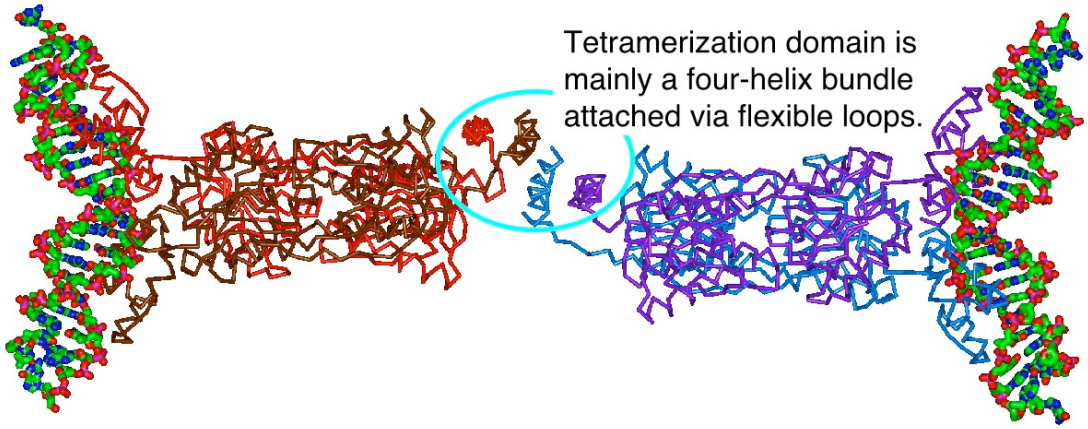

J. Kahn

Rationalizing Two Populations

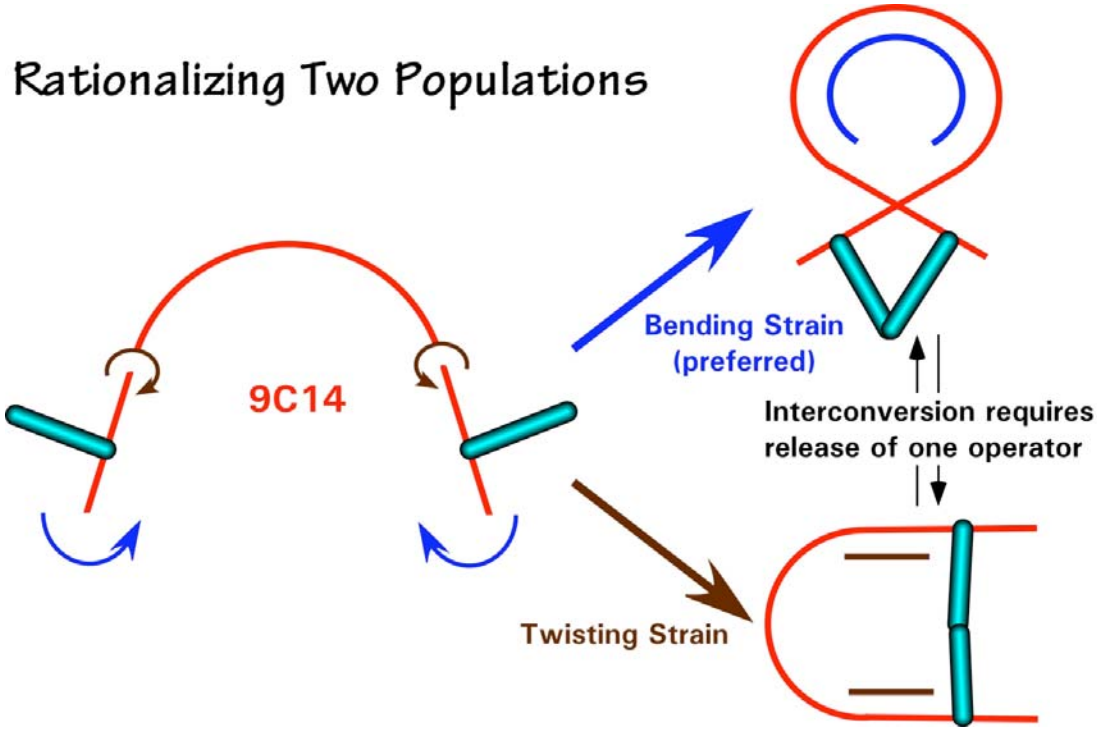

J. Kahn

Test using physical methods !

J. Kahn

Förster Theory for Fluorescence Resonance Energy Transfer

- The efficiency of energy transfer *E* from a donor fluorophore to an acceptor can be used to measure the distance between fluorophores.
- *E* can be measured from quenching of donor fluorescence or a decreased fluorescence lifetime in the presence of acceptor. Both result from the additional transfer decay path.
- We can also measure sensitized emission of the acceptor in the presence of donor. This is useful because it helps distinguish between energy transfer and simple quenching.

J. Kahn

Distance Dependence of FRET

- (After Selvin, 1996)
- FRET is a transition dipole-transition dipole interaction. The Hamiltonian is:

$$H = \frac{\mu_A \bullet \mu_D}{R^3} - \frac{(\mu_A \bullet \mathbf{R})(\mu_D \bullet \mathbf{R})}{R^5}$$

- Fermi's Golden Rule: the rate of energy transfer is proportional to the square of the matrix element:

$$k_T \propto \left[\langle D^* A | H | DA^* \rangle\right]^2 \propto \frac{\kappa^2}{R^6}$$

- We absorb the orientation dependence into the infamous κ^2 factor, where $0 < \kappa^2 < 4$ and we assume it averages to $^2/_3$. This is why most applications of FRET give only relative numbers.
- The overlap between the D*A and DA* wave functions leads to an integral over the emission spectrum of the donor and the absorption spectrum of the acceptor. The quantum yield of the donor enters in because it reflects the probability of donor de-excitation by other pathways. This gives:

J. Kahn

Fluorescence Resonance Energy Transfer (FRET) Principles

Phenomenon and Geometric Factors

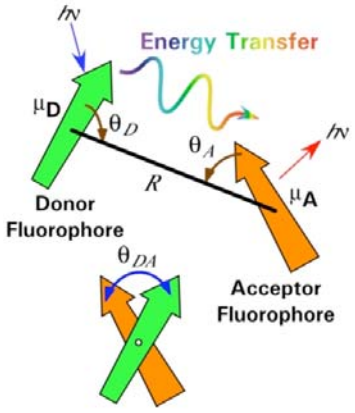

$\kappa^2 = (\cos\theta_{DA} - 3\cos\theta_A \cos\theta_D)^2$

$= 2/3$ for random orientations

Spectral Overlap

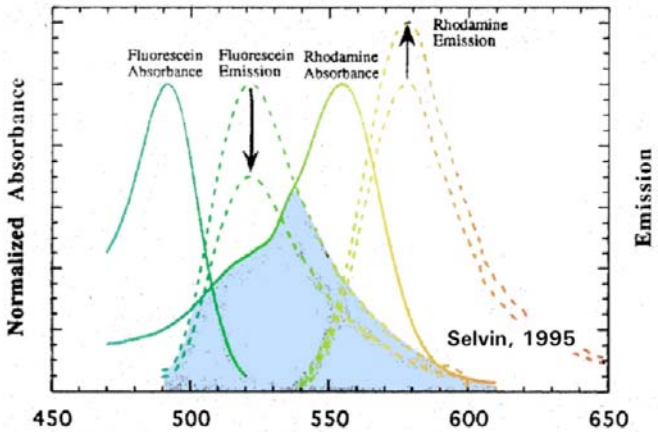

$J = \int \varepsilon_A(\lambda) f_D(\lambda) \lambda^4 \, d\lambda$

$R_0 = 8.79 \times 10^{-5} \left(J \kappa^2 n^{-4} \Phi_D\right)^{1/6}$ Å constant for random orientations for a given D-A pair

Bottom Line:

1. **Measure transfer efficiency (donor quenching or stimulated acceptor emission).**
2. **Calculate distance:** $E = R_0^6 / \left(R_0^6 + R^6\right)$ $R = R_0 \left[(1-E)/E\right]^{1/6}$

J. Kahn

Verification of Hyperstable Loop Geometry: Fluorescence Resonance Energy Transfer

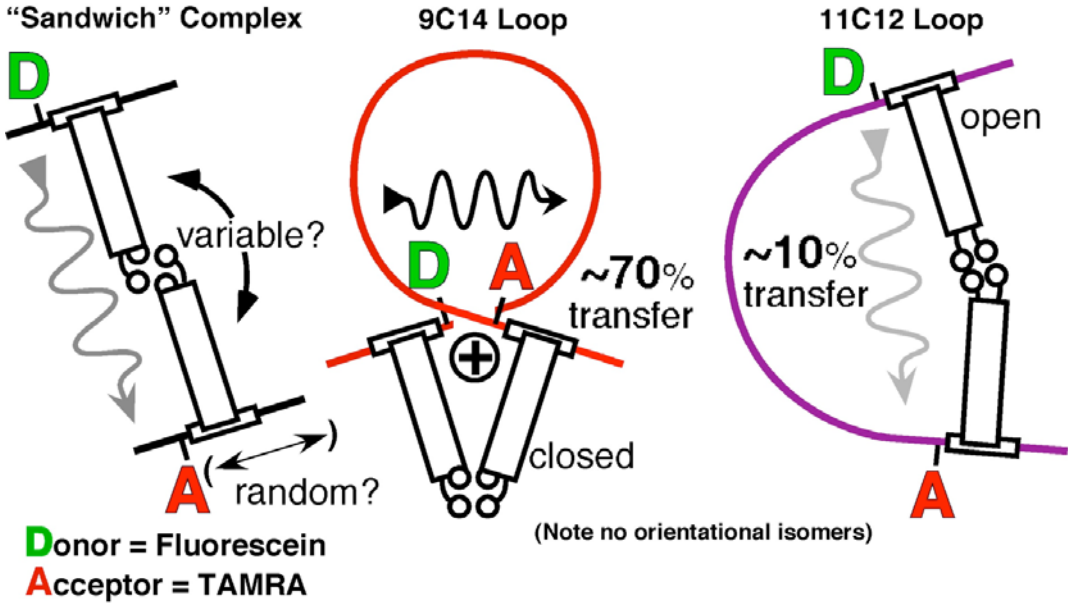

J. Kahn

Doubly-labeled Constructs Used for FRET Experiments

Fluorophores are attached in the major groove away from LacI, ~130 bp or ~ 400Å apart along the DNA contour

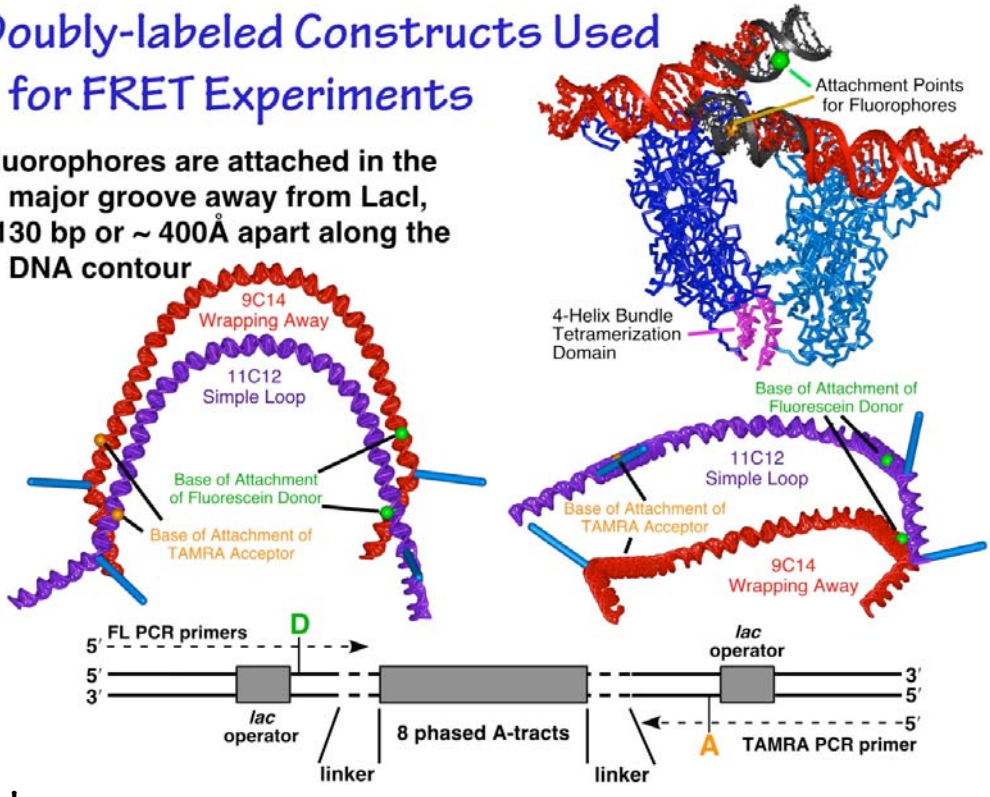

J. Kahn

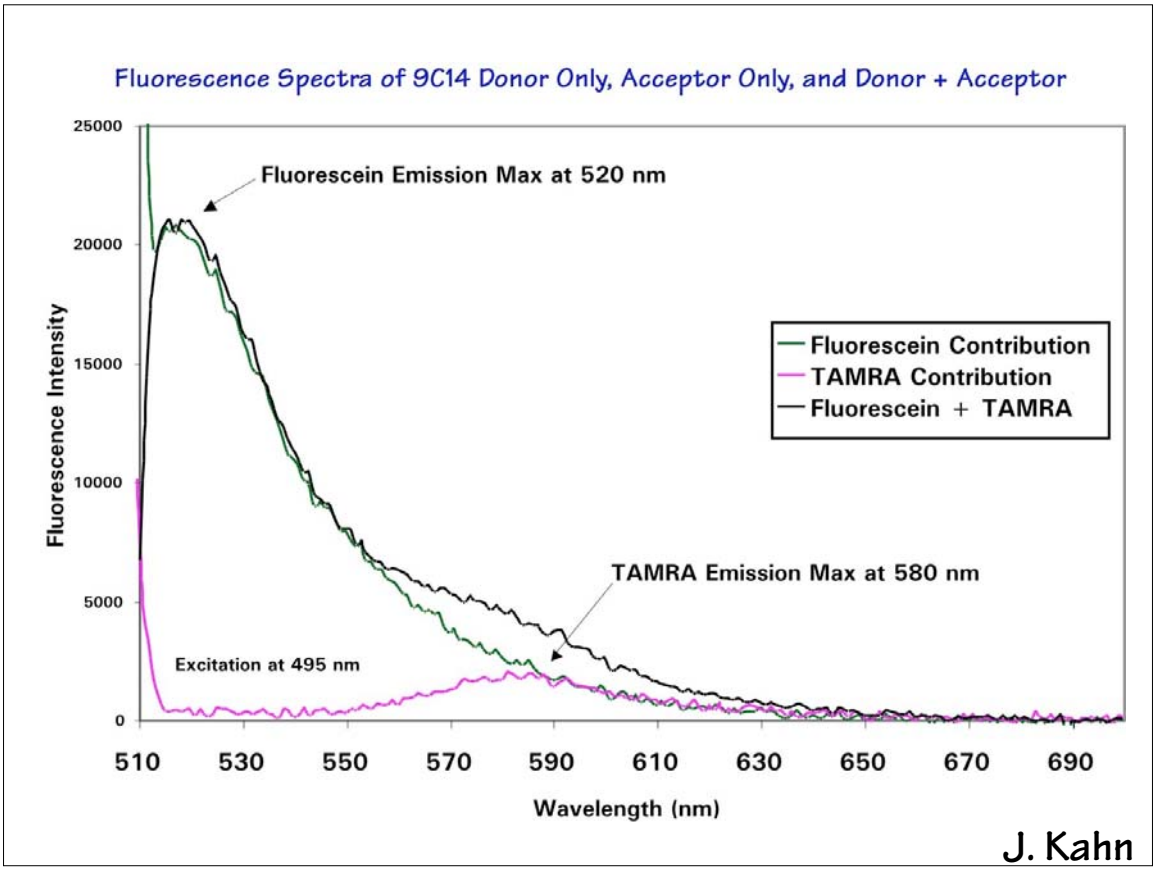
Fluorescence Spectra of 9C14 Donor Only, Acceptor Only, and Donor + Acceptor
Fluorescein Emission Max at 520 nm
TAMRA Emission Max at 580 nm
Excitation at 495 nm
Fluorescein Contribution
TAMRA Contribution
Fluorescein + TAMRA
Fluorescence Intensity
Wavelength (nm)
25000
20000
15000
10000
5000
0
510
530
550
570
590
610
630
650
670
690
J. Kahn

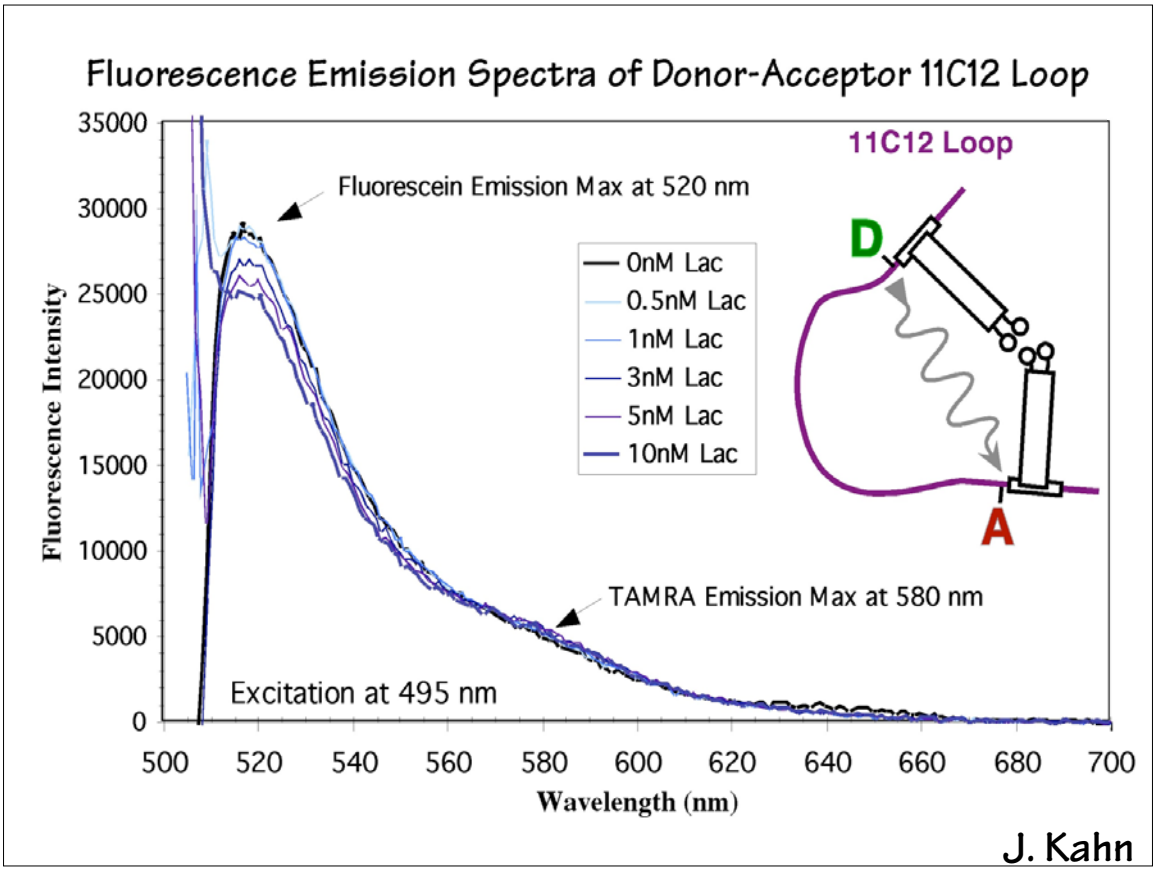
Fluorescence Emission Spectra of Donor-Acceptor 11C12 Loop
11C12 Loop
D
A
Fluorescein Emission Max at 520 nm
TAMRA Emission Max at 580 nm
Excitation at 495 nm
0nM Lac
0.5nM Lac
1nM Lac
3nM Lac
5nM Lac
10nM Lac
Fluorescence Intensity
Wavelength (nm)
35000
30000
25000
20000
15000
10000
5000
0
500
520
540
560
580
600
620
640
660
680
700
J. Kahn

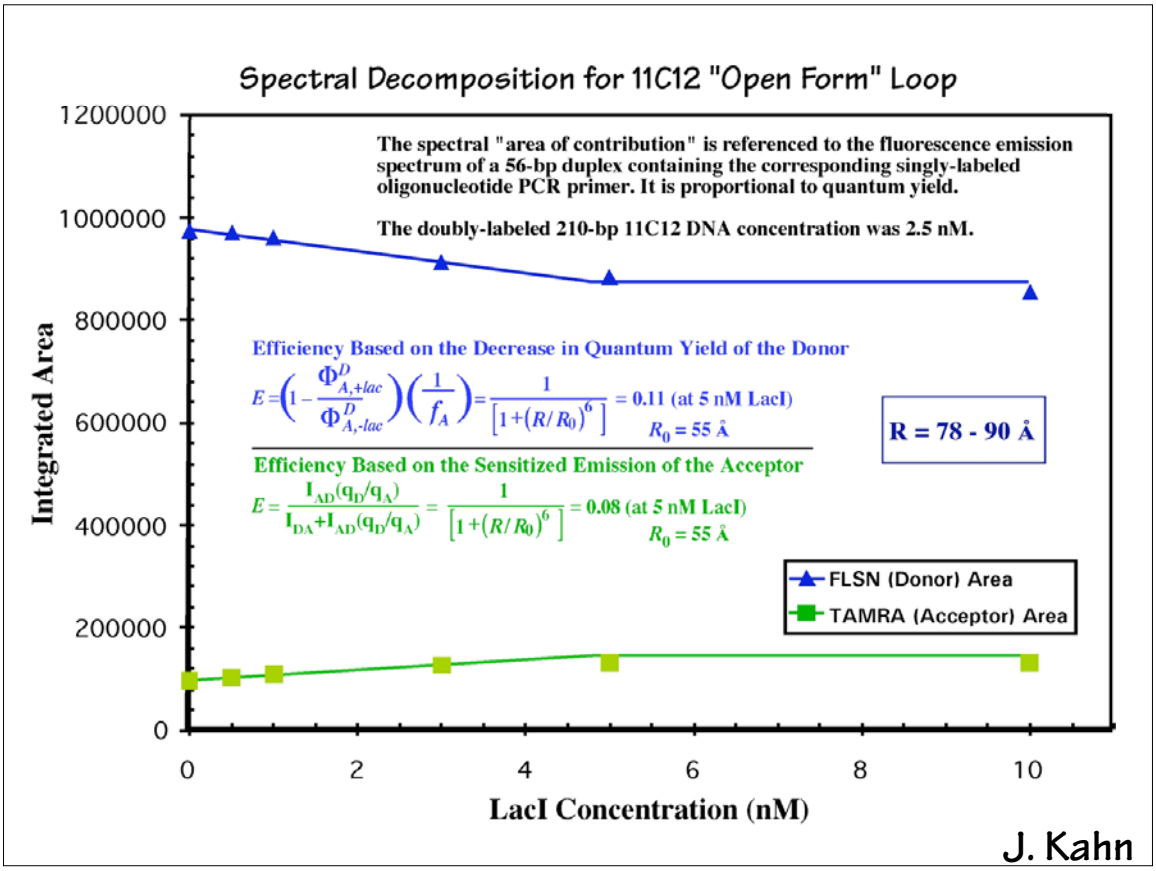
Spectral Decomposition for 11C12 "Open Form" Loop
The spectral "area of contribution" is referenced to the fluorescence emission spectrum of a 56-bp duplex containing the corresponding singly-labeled oligonucleotide PCR primer. It is proportional to quantum yield.
The doubly-labeled 210-bp 11C12 DNA concentration was 2.5 nM.
Efficiency Based on the Decrease in Quantum Yield of the Donor
$E = \left(1 - \frac{\Phi^D_{A,+lac}}{\Phi^D_{A,-lac}}\right)\left(\frac{1}{f_A}\right) = \frac{1}{\left[1+(R/R_0)^6\right]}$ = 0.11 (at 5 nM LacI) R_0 = 55 Å
R = 78 - 90 Å
Efficiency Based on the Sensitized Emission of the Acceptor
$E = \frac{I_{AD}(q_D/q_A)}{I_{DA}+I_{AD}(q_D/q_A)} = \frac{1}{\left[1+(R/R_0)^6\right]}$ = 0.08 (at 5 nM LacI) R_0 = 55 Å
FLSN (Donor) Area
TAMRA (Acceptor) Area
Integrated Area
1200000
1000000
800000
600000
400000
200000
0
0
2
4
6
8
10
LacI Concentration (nM)
J. Kahn

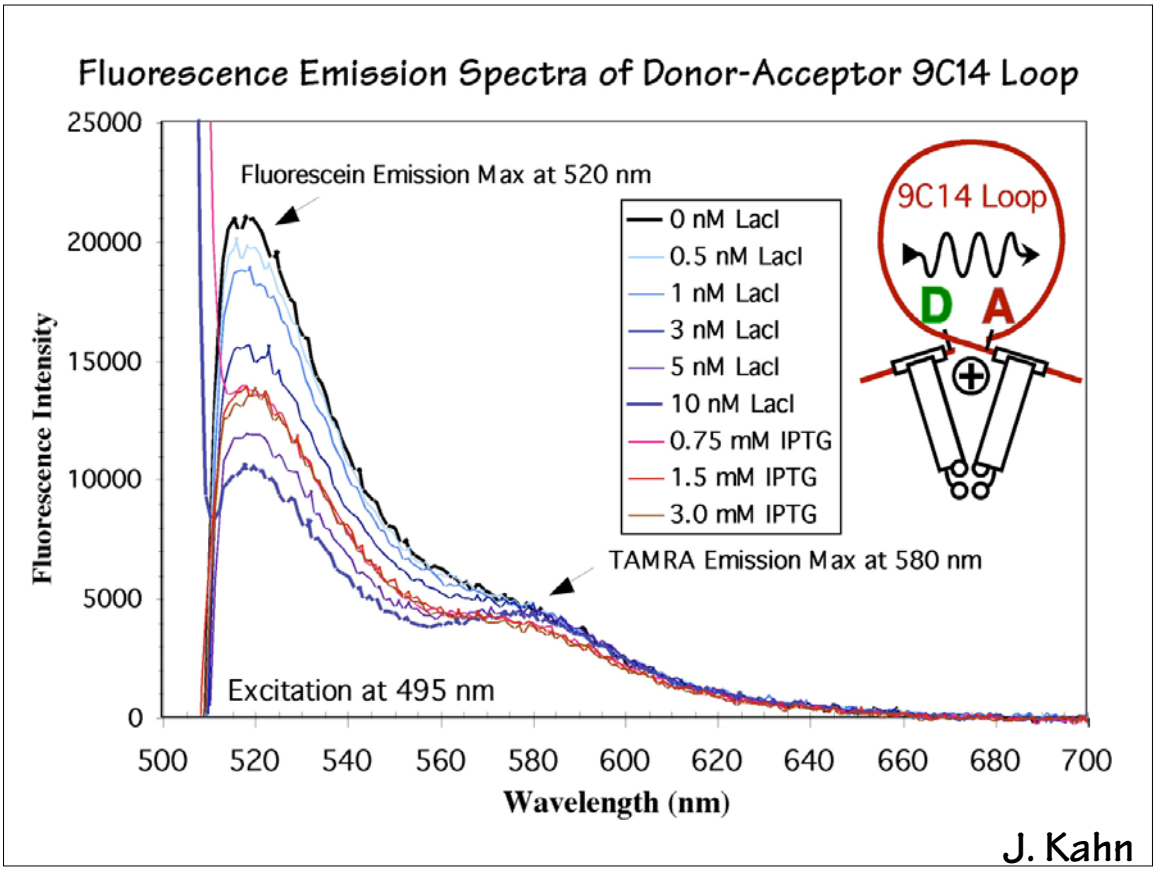
Fluorescence Emission Spectra of Donor-Acceptor 9C14 Loop
Fluorescein Emission Max at 520 nm
TAMRA Emission Max at 580 nm
Excitation at 495 nm
0 nM LacI
0.5 nM LacI
1 nM LacI
3 nM LacI
5 nM LacI
10 nM LacI
0.75 mM IPTG
1.5 mM IPTG
3.0 mM IPTG
9C14 Loop
D
A
Fluorescence Intensity
25000
20000
15000
10000
5000
0
500
520
540
560
580
600
620
640
660
680
700
Wavelength (nm)
J. Kahn

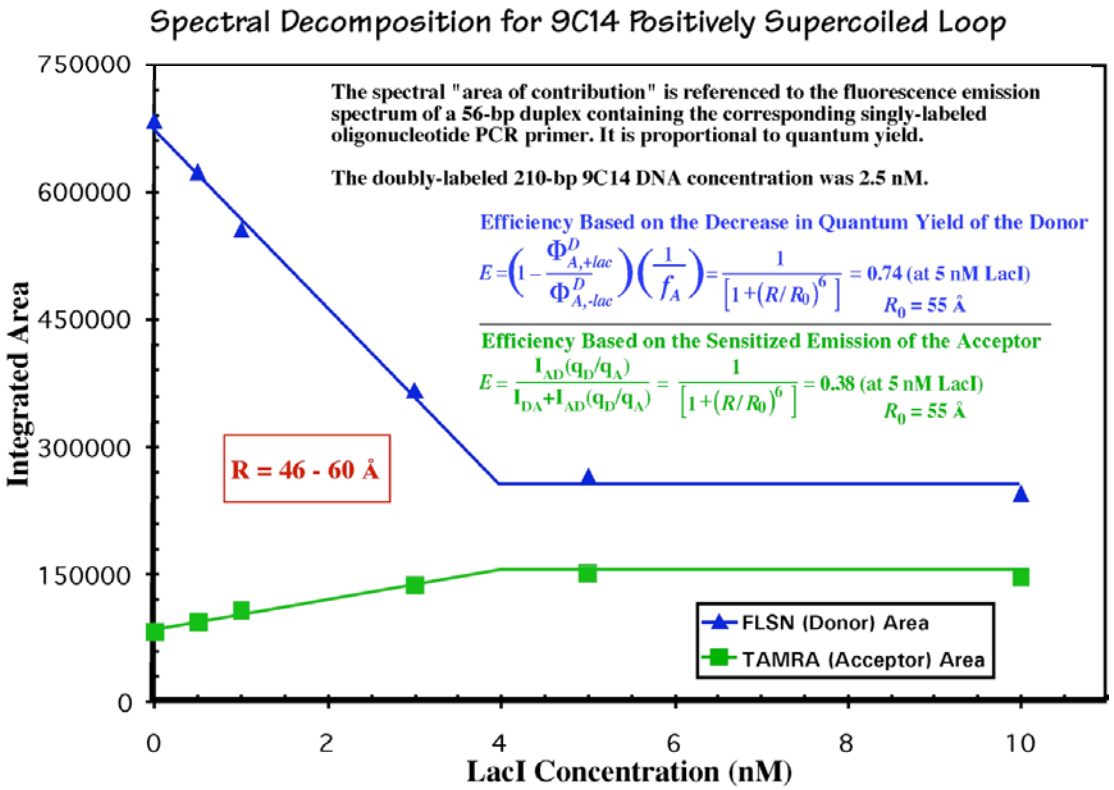

J. Kahn

Control Experiments

- Restriction digestion analysis shows that there is no energy transfer for either construct in the absence of Lac repressor.
- Electrophoretic mobility shift experiments show complete binding of fluorescent DNA.
- Experiments on singly-labeled DNA show that fluorescein and TAMRA emission are each quenched only 0-5% by repressor binding.
- IPTG does not significantly quench either fluorophore in singly-labeled DNA.
- But…in retrospect we could have been more careful about repeated measurements of the TAMRA labeling efficiency.

J. Kahn

Photon Accounting

- Why does energy transfer appear less efficient for acceptor emission vs. donor quenching?
- Excitation spectra show that there is significant LacI-induced quenching of TAMRA, but **only** in the double-labeled molecule! (Confirmed by emission spectra with excitation at 560 nm.) This explains why the overall TAMRA emission is lower than expected.
- Spectral decomposition of excitation spectra shows that the FL contribution at the TAMRA emission maximum remains constant, even though FL is substantially quenched overall. This suggests that energy transfer from FL to TAMRA is quite efficient, which leads to an excitation spectrum component from FL appearing with an emission spectrum characteristic of TAMRA.
- **Conclusion:** FL probe perturbs TAMRA photophysics: via allostery? Exciton coupling? Electrostatics? Does the converse also occur?

J. Kahn

Fluorescence Excitation Spectra of Donor-Acceptor 9C14 Loop

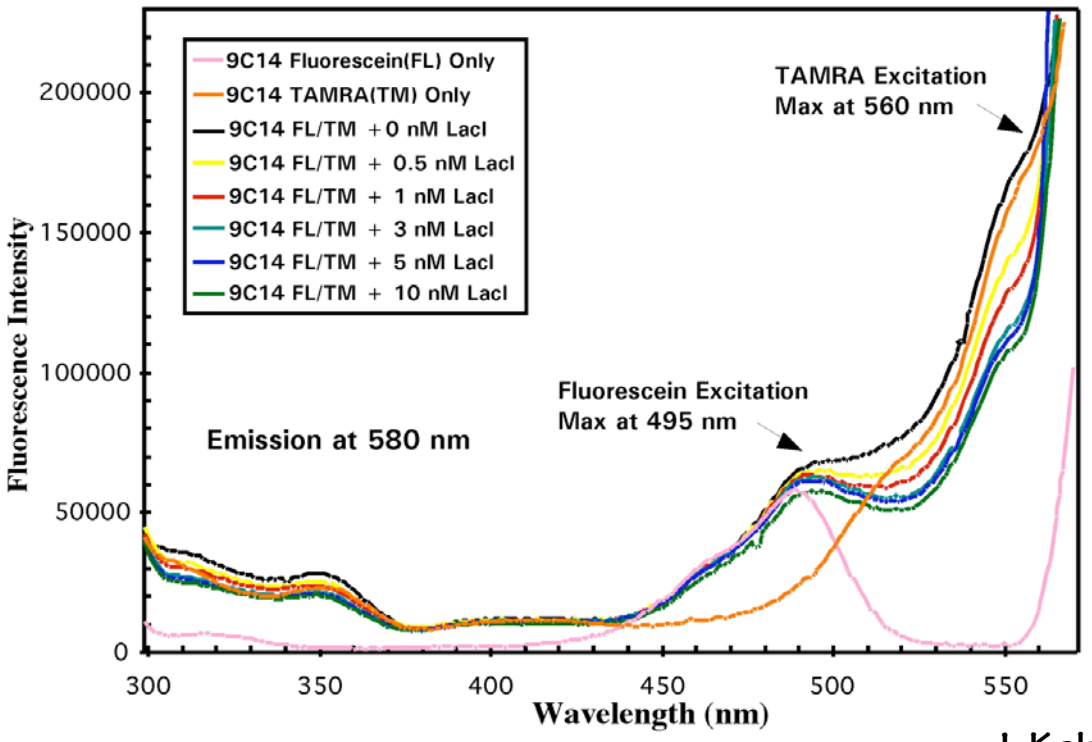

J. Kahn

Spectral Decomposition for the Excitation Spectra of the 9C14 Positively Supercoiled Loop

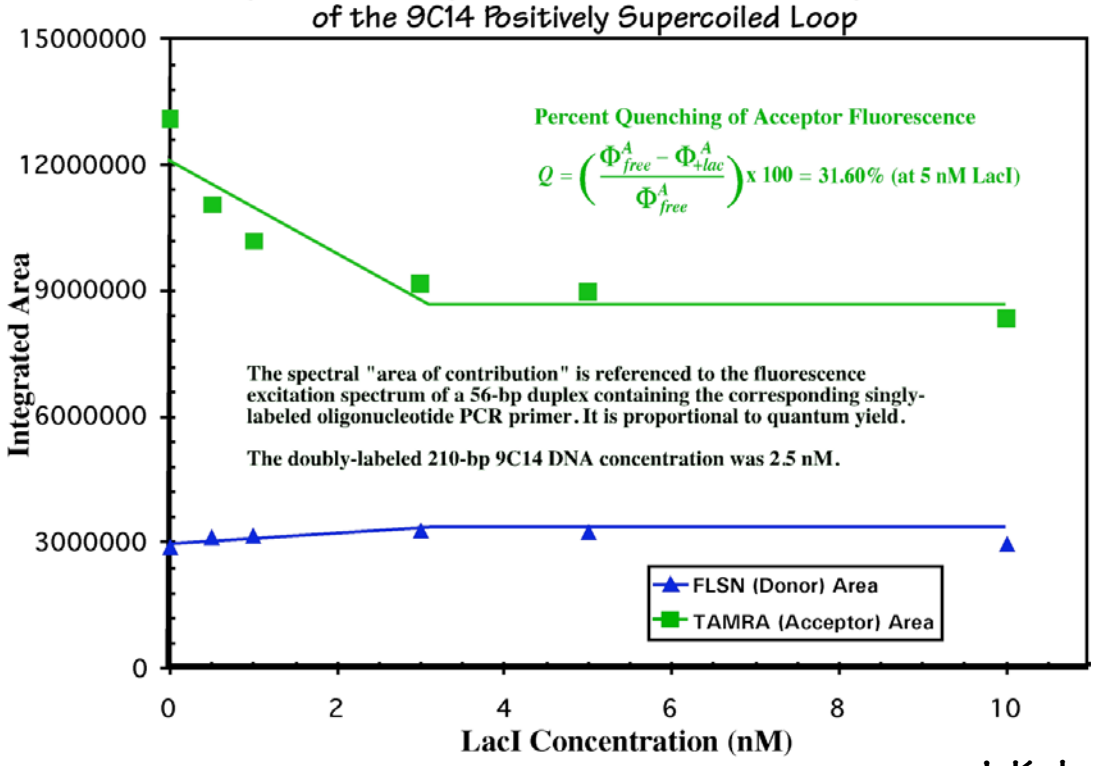

J. Kahn

Correction of Efficiency Calculated by Sensitized Emission

Fractional Quenching of Acceptor Fluorescence

Calculated from:

Q_{ex} = 9C14 Donor/Acceptor Excitation Spectra = 0.3160

(*ex:* 300-575 nm; *em:* 580 nm)

Q_{em} = 9C14 Donor/Acceptor Emission Spectra = 0.1812

(*ex:* 560 nm; *em:* 565-700 nm)

Q_{AV} = 0.2486

Uncorrected Efficiency Based on the Sensitized Emission of the Acceptor

$$E_{uncorrected} = \frac{\left(I_{A,+lac} - I_{A,-lac}\right)\left(\frac{q_D}{q_A}\right)}{I_{D,+lac} + \left(I_{A,+lac} - I_{A,-lac}\right)\left(\frac{q_D}{q_A}\right)} = 0.382$$

Corrected Efficiency Based on the Sensitized Emission of the Acceptor

$$E_{corrected} = \frac{\left[I_{A,+lac} - I_{A,-lac}(1-Q_{AV})\right]\left[\frac{q_D}{q_A(1-Q_{AV})}\right]}{I_{D,+lac} + \left[I_{A,+lac} - I_{A,-lac}(1-Q_{AV})\right]\left[\frac{q_D}{q_A(1-Q_{AV})}\right]} = 0.516$$

Summary of Efficiency and Distance Calculations

Method	Efficiency (E)	Distance (Å)
Decrease in Quantum Yield of the Donor	0.738	46.3
Corrected Sensitized Emission of the Acceptor	0.516	54.4

J. Kahn

Proposed Intermediate Opening Geometries

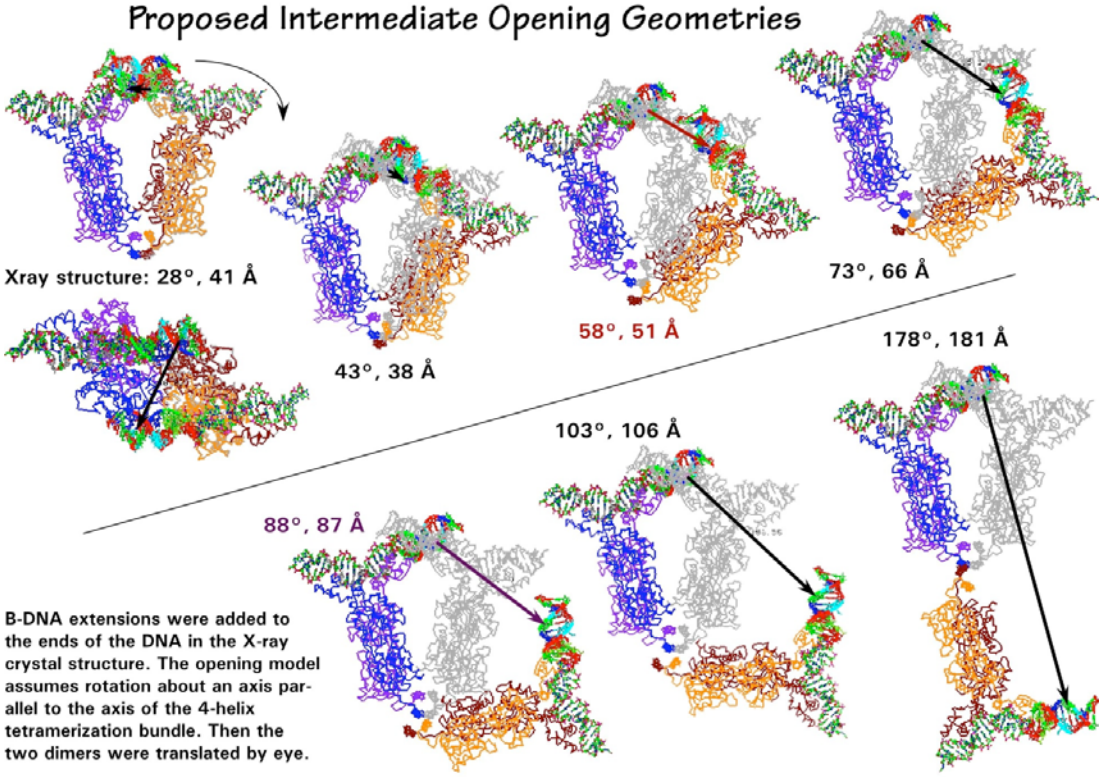

B-DNA extensions were added to the ends of the DNA in the X-ray crystal structure. The opening model assumes rotation about an axis parallel to the axis of the 4-helix tetramerization bundle. Then the two dimers were translated by eye.

J. Kahn

Time-resolved Fluorescence

- Laser excitation at 335 nm, time-resolved photon counting using a monochromator and microchannel plate detector, channel width 47 ps.
- Detection at 515 nm monitors fluorescein donor lifetime.
- Best global fit to data was obtained with four consistent lifetimes and variable amplitudes, as shown.
- Even at saturation some FL remains unperturbed. Suggests two populations, one which transfers very rapidly, one with unaffected lifetime? Closed and open forms?
- 0.6 ns transient is puzzling: although very close to expected value for E = 80 %, why is it there for free DNA?

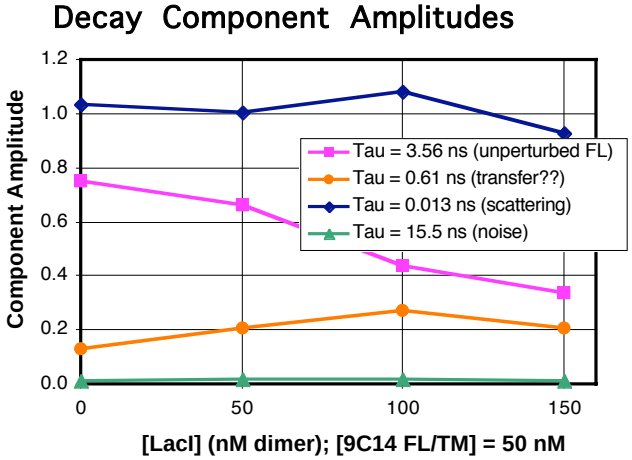

John J. Harvey and Jay R. Knutson, NHLBI, NIH

J. Kahn

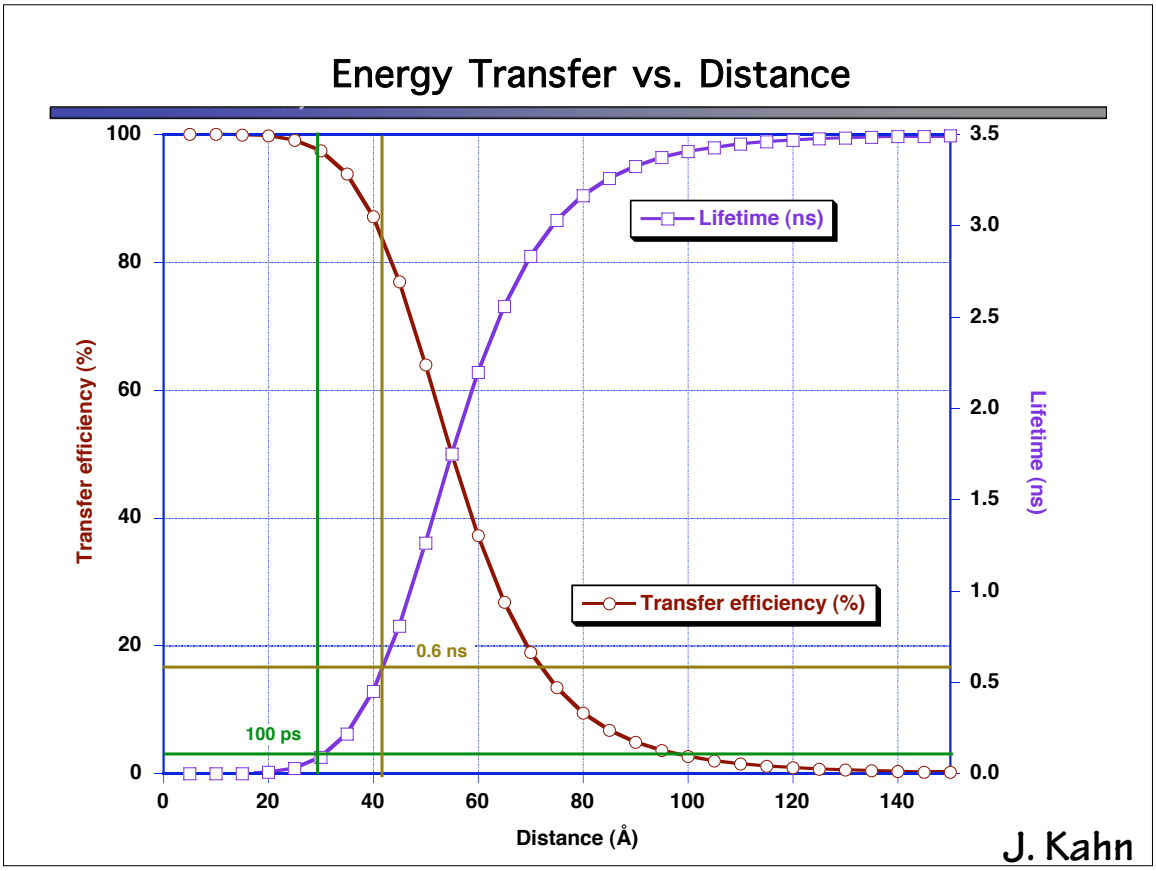
Energy Transfer vs. Distance
Transfer efficiency (%)
Lifetime (ns)
Distance (Å)
Lifetime (ns)
Transfer efficiency (%)
0.6 ns
100 ps
J. Kahn

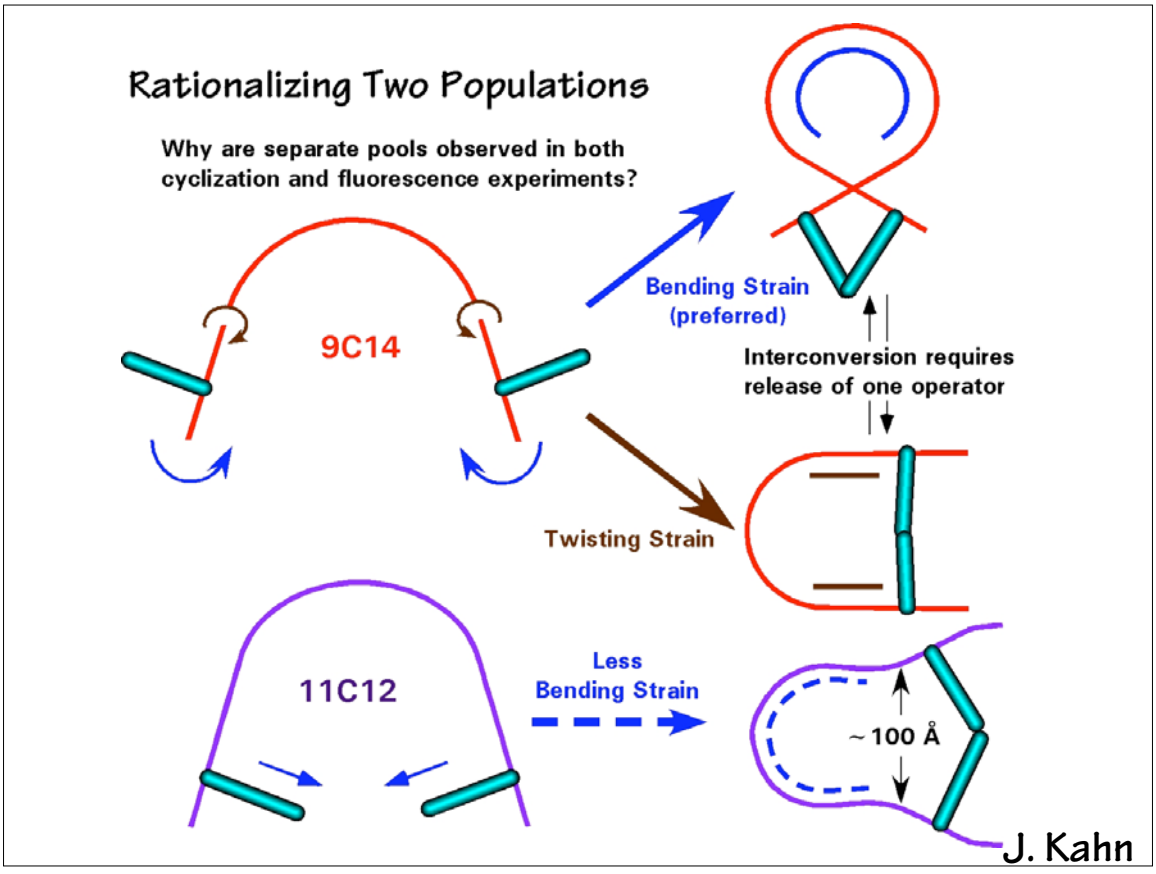
Rationalizing Two Populations
Why are separate pools observed in both cyclization and fluorescence experiments?
9C14
Bending Strain (preferred)
Interconversion requires release of one operator
Twisting Strain
11C12
Less Bending Strain
~100 Å
J. Kahn

FRET Conclusions and Prospects

- First demonstration of energy transfer in a DNA loop.
- FRET experiments confirm the flexibility of Lac repressor and the idea of open and closed loop shapes.
- Preliminary evidence suggestive of mixed populations obtained from lifetime measurements. Is it real?
- Edelman, Cheong, and Kahn, Biophys. J. 2003

J. Kahn

Theoretical Framework for DNA Looping

Monte Carlo programs for simulating loop conformation were adapted from DNA ring closure methods: Simulate half-chains originating at lacO, filter for end closure

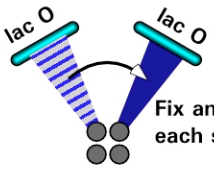

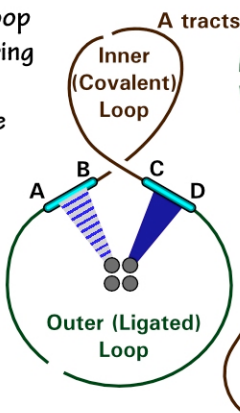

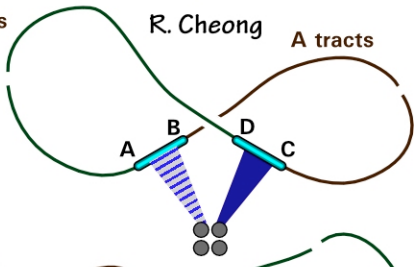

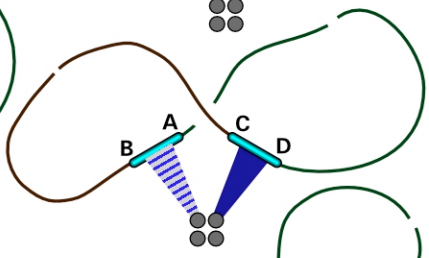

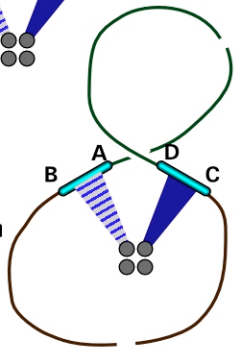

All four loop types must be considered

Inner loop J factors and protein deformation energy are converted to free energy of each DNA loop type

Inner loop stability determines loop population distribution

Only inner loop is needed to compare to FRET

Inner and outer distributions are melded to make complete loop population

Weighted average outer loop J factor is compared to experiment

Topological distribution determined, compared to experiment

Simulations of FRET molecules

- Simulations correctly predict relative energy transfer efficiencies

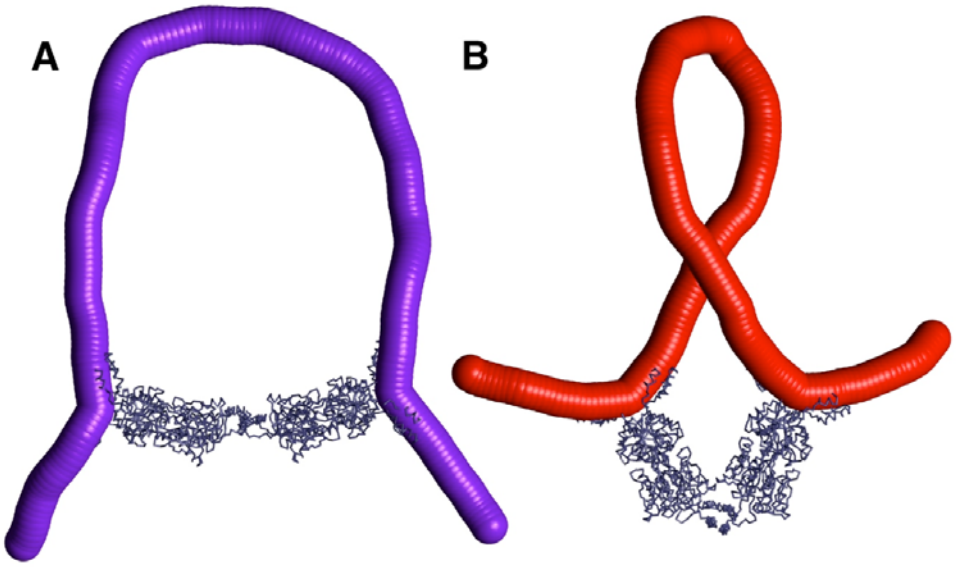

J. Kahn

Simulated LacI-DNA Loops

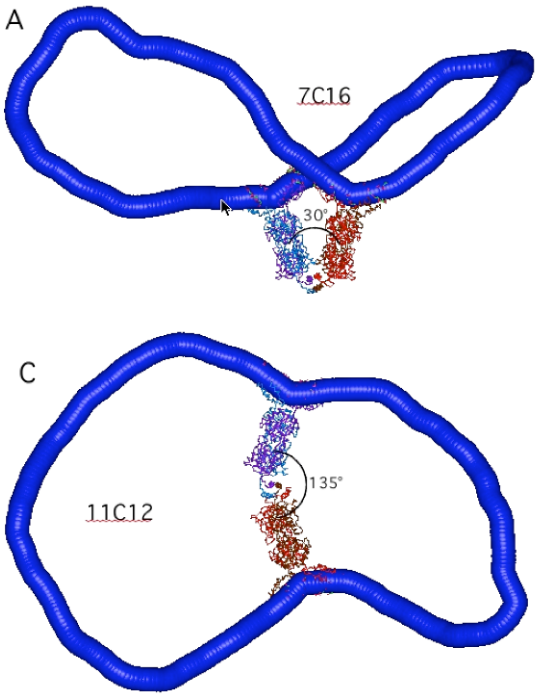

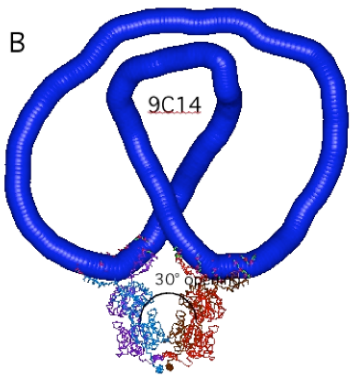

Loops shown were generated using Monte Carlo methods by filtering random DNA chains for closed-loop shapes. Bound LacI imposed an additional geometric constraint. Results indicate two modes of LacI opening: small LacI angles where ΔLk = -1 (A) and ΔLk = +1 (B) topoisomers dominate, or large LacI angles where ΔLk = 0 (C) topoisomers dominate.

J. Kahn

Simulations Match Experimental Topoisomer Distributions

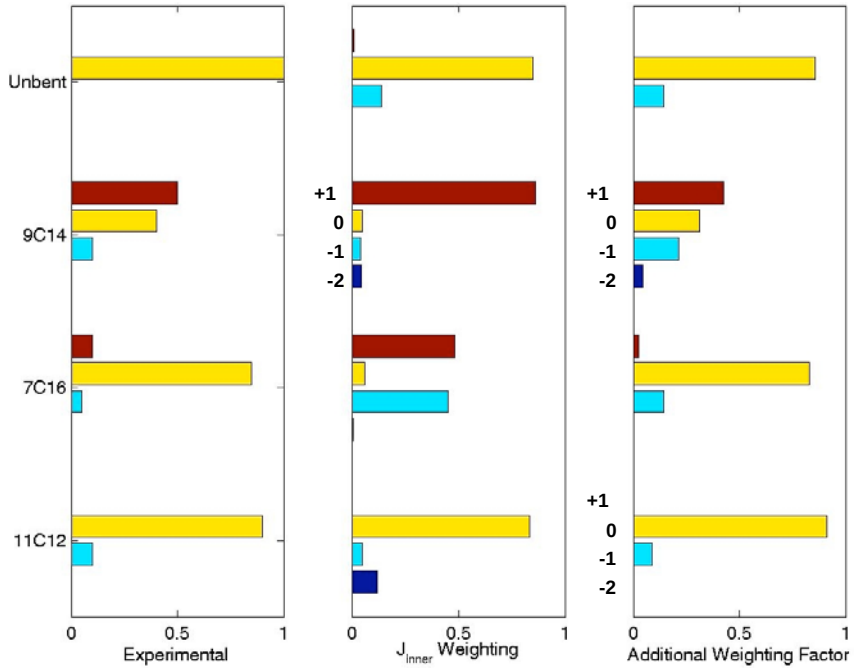

J. Kahn

Simulations require imposing a preference for open form loop

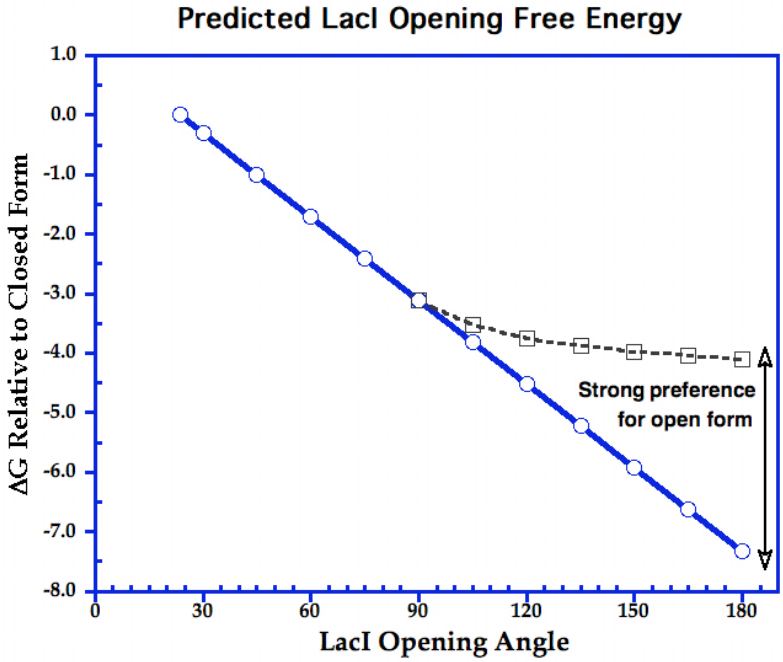

J. Kahn

Biological Implications

- Efficient repression (unlike activation…) requires nearly complete site occupancy.
- Changes in cellular cation concentrations, and/or the binding of specific or non-specific DNA bending proteins, change DNA shape and flexibility.
- The flexibility of Lac repressor (and probably others, like AraC: Schleif) allows it to bind efficiently under different DNA bending/flexibility conditions, although not at different helical phasing (Record; Müller-Hill).
- Similar activation mechanisms (flexibility, multivalency) have evolved for evading the constraints of DNA physical chemistry, including twist constraints (Maher; Lilja and Kahn).

J. Kahn

Overall Conclusions and Open Questions

- Biochemical experiments show that DNA can be designed to form hyperstable loops with Lac repressor.
- FRET experiments confirm Lac repressor flexibility, choice of open and closed loop shapes.
- Protein flexibility may allow efficient repression (and activation) under a variety of conditions.

- Can the 9C14-LacI loop assume two forms?
- What do we really know about the geometries?
- Can we use what we have learned from these systems to design protein-DNA loops and other structures?

J. Kahn

Single-Molecule FRET on LacI-9C14

- Collaboration with Doug English's group, Chemistry and Biochemistry, UMCP
- Goals: What do we get from single molecules that we don't already know?
  - Characterize population distributions rather than averages: are there two loop types?
  - Measure ET for the individual populations
  - Measure interconversion rates (requires immobilization)
  - Observe rare events
- Michael Morgan

J. Kahn

Single-Molecule Apparatus and Data

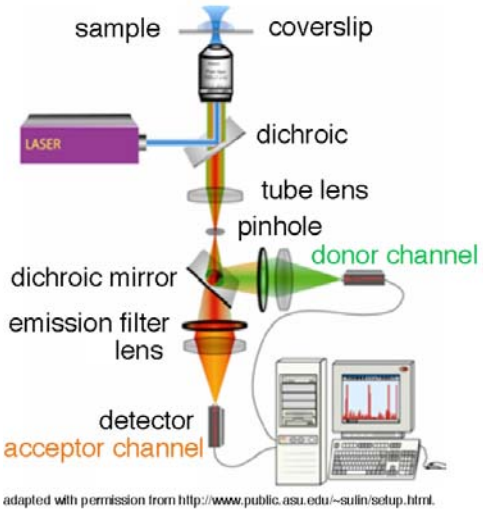

adapted with permission from http://www.public.asu.edu/~sulin/setup.html.

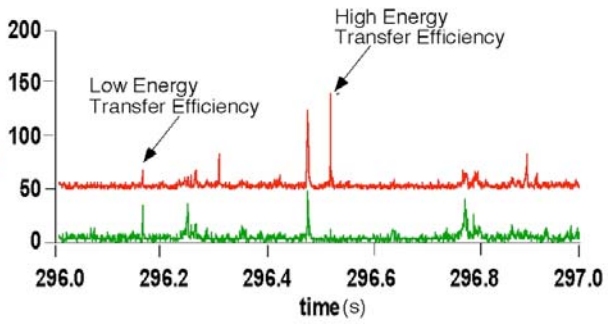

Calculate Efficiency of Energy Transfer (ET) = $\frac{I_A}{I_A + I_D}$
(corrected for Donor leak-through)

J. Kahn

Single Molecule-Titration Experiments

1.25nM DNA **0.0 nM LacI**

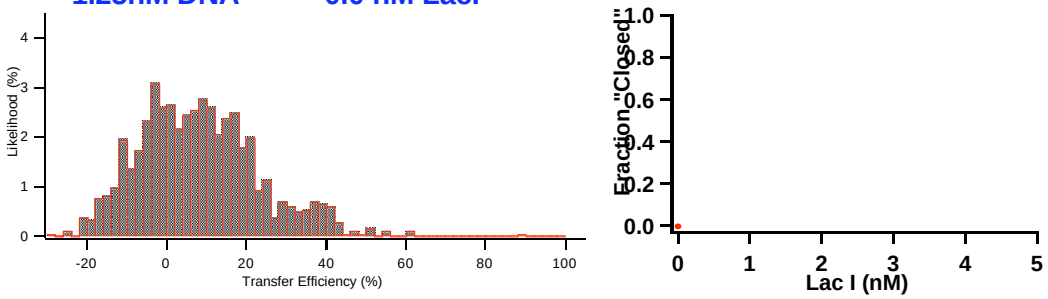

- **The free DNA shows no evidence of efficient energy transfer. The "zero-ET peak" is broadened by noise from donor leakage correction.**

J. Kahn

Single Molecule-Titration Experiments

1.25nM DNA **0.05 nM LacI**

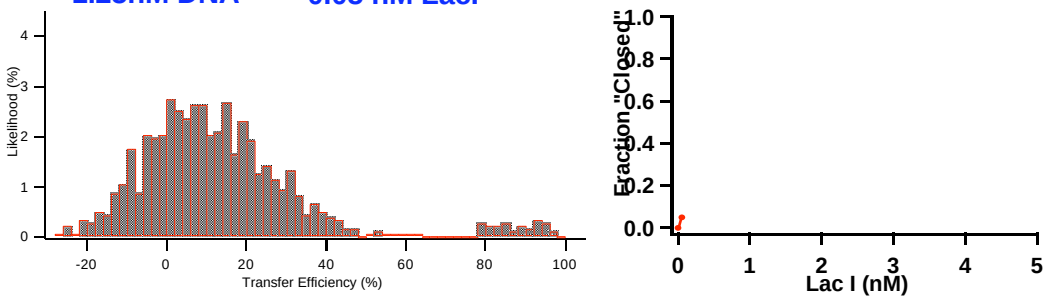

- **As LacI is titrated in a population exhibiting nearly 100 % energy transfer efficiency appears**

J. Kahn

Single Molecule-Titration Experiments

1.25nM DNA **0.5 nM LacI**

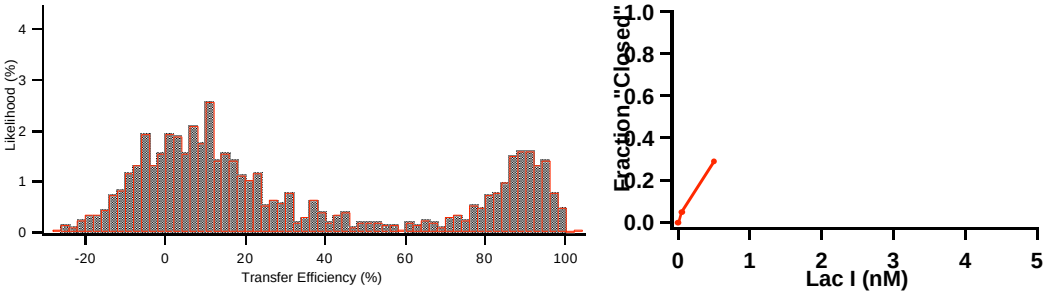

- **As LacI is titrated in a population exhibiting nearly 100 % energy transfer efficiency appears**

J. Kahn

Single Molecule-Titration Experiments

1.25nM DNA **2.5 nM LacI**

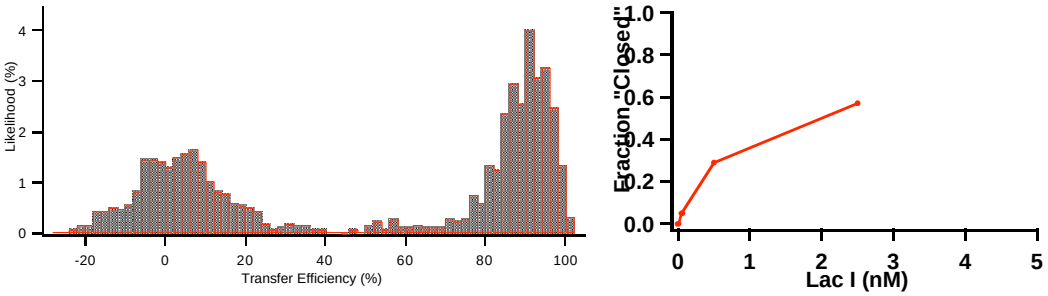

- **As LacI is titrated in a population exhibiting nearly 100 % energy transfer efficiency appears**
  - **The effect saturates at ≤ 2.5 nM LacI, suggesting nearly stoichiometric binding.**
  - **A substantial population (40%) remains in the "zero-ET peak" of the histogram obtained at saturation.**
    (Possible explanation for the 70% ET observed in bulk FRET experiments)

J. Kahn

Single Molecule-Titration Experiments

1.25nM DNA **5.0 nM LacI**

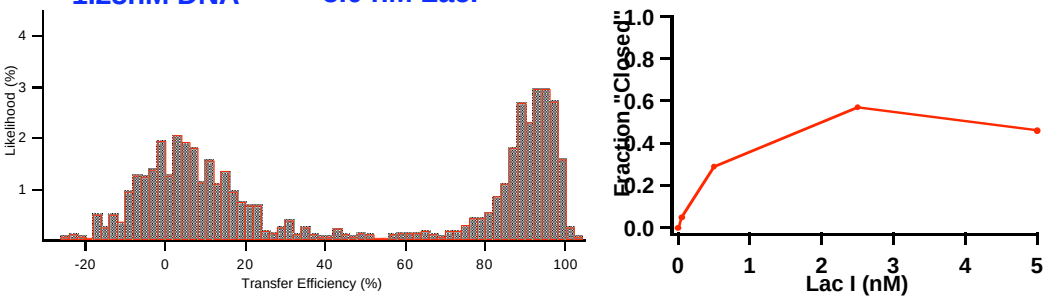

- As LacI is titrated in a population exhibiting nearly 100 % energy transfer efficiency appears. We see almost no examples of the 70 % average behavior!
  - The effect saturates at ≤ 2.5 nM LacI, suggesting nearly stoichiometric binding.
  - A substantial population (40%) remains in the "zero-ET peak" of the histogram obtained at saturation.
    (Possible explanation for the 70% ET observed in bulk FRET experiments)

J. Kahn

Single Molecule-Titration Experiments

1.25nM DNA **0.0 nM LacI**

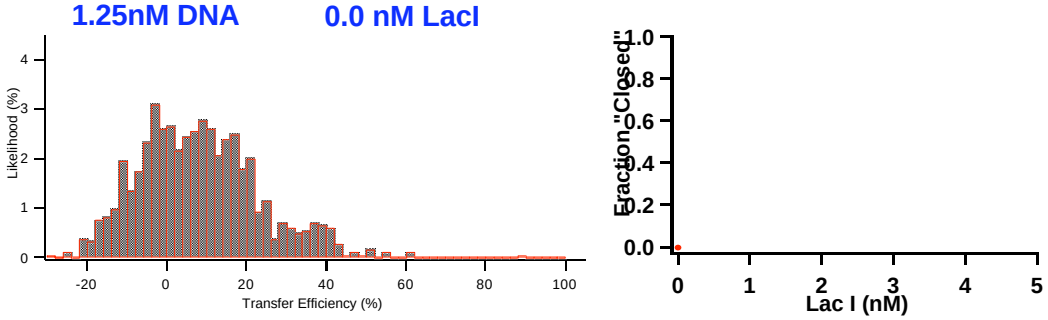

- Still not clear what comprises the zero-ET peak.

J. Kahn

Laser Excitation Power Dependence of Observed SM-FRET

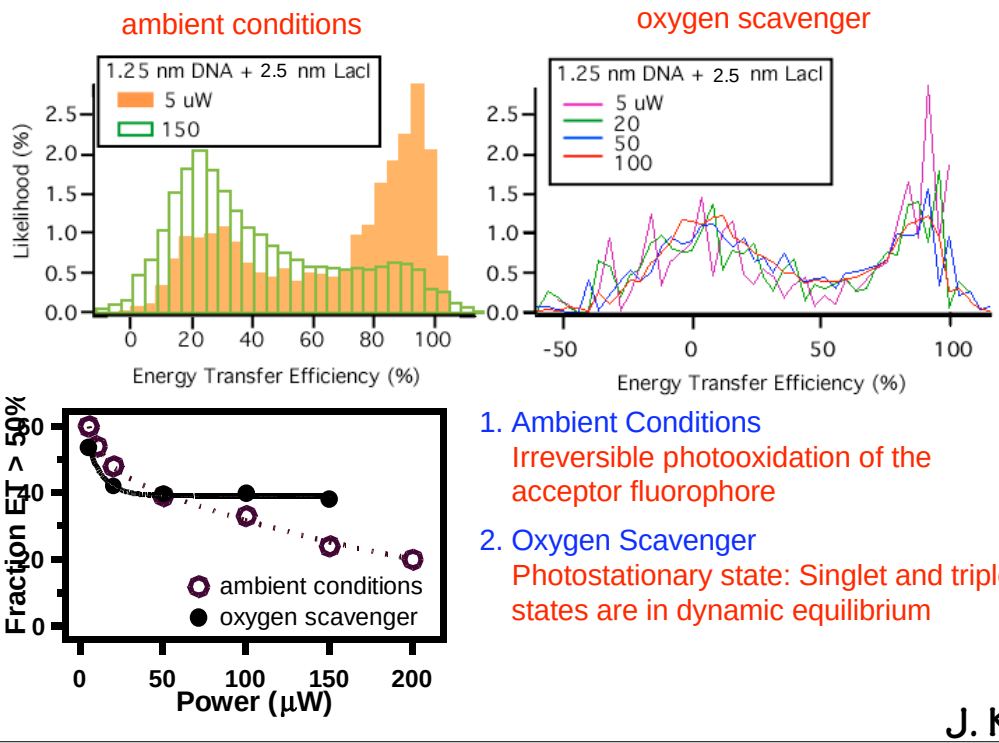

1. Ambient Conditions
   Irreversible photooxidation of the acceptor fluorophore
2. Oxygen Scavenger
   Photostationary state: Singlet and triplet states are in dynamic equilibrium

J. Kahn

Tentative Photophysics of Acceptor Triplet State

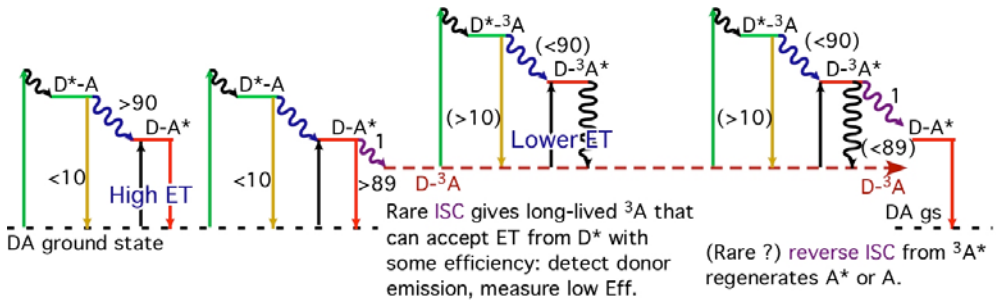

- The most common event is energy transfer from D* to A followed by acceptor fluorescence, but occasionally A* converts to ^{3}A.
- D*-^{3}A must emit some fluorescence, because otherwise the state would be dark and could not affect the observed transfer.
- R_0 is probably shorter (less efficient transfer) for D-^{3}A than for D-A due to decreased spectral overlap for the D-^{3}A pair, so we observe some donor fluorescence. ^{3}A* is presumably nonemissive but this is not required if R_0 is shorter for D-^{3}A, so we observe a lower-ET state.
- There is precedent (Tinnefeld *et al.*, 2003) for a triplet state acting as an energy transfer acceptor.

J. Kahn

How Does D-^{3}A Transfer Explain the Power Dependence?

- Low power: D-^{3}A typically does not form. If it does, it does not absorb another photon during the illumination time, so >90% ET is observed.
- Intermediate power: If D-^{3}A forms, we observe *Eff* < 90 % because there are some donor emission events from D*-^{3}A before it diffuses out of the beam: *Eff* decreases but not as much as at high power.
- High power: Observe *Eff* < 90 % because of donor emission from D*-^{3}A. The plateau at high power suggests that there must be a mechanism to regenerate A: otherwise suppression of ET by long-lived ^{3}A would continue to increase with power above 50 μW. Reverse ISC frequently occurs before the molecule diffuses out of the beam. At high flux a statistical distribution of all the events shown occurs during the illumination time.
- Any mechanism for light-dependent regeneration of ground state A could explain the data. If ^{3}A relaxed spontaneously, then we would expect more donor emission during its lifetime at higher flux, hence a progressive decrease in measured *Eff* as power increases.
- The model can also explain the ambient power dependence assuming rapid triplet relaxation by O_2, with or without irreversible bleaching by $^1O_2$.

J. Kahn

Dealing with Donor and Acceptor Photobleaching and Mislabeling

There are many mislabeled molecules in our SMS experiments

Donor + Acceptor	Capable of ET
Donor-only	Incapable of ET, shows up in "zero-ET peak"
Acceptor-only	Incapable of ET, however if directly excited can show up as weak ET
9C14-unlabeled	Invisible to the microscope

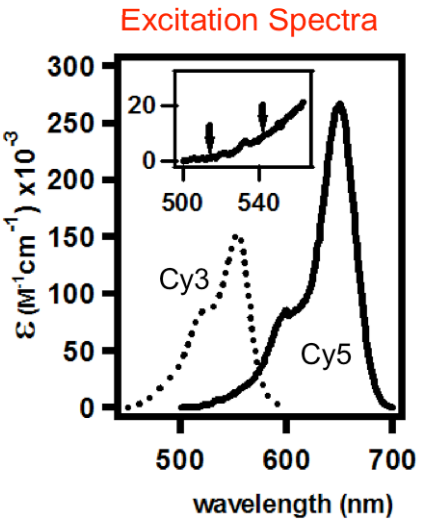

J. Kahn

Excitation at Two Different Wavelengths

514nm

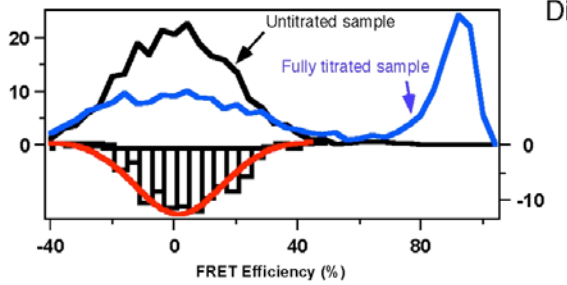

Direct excitation of the donor with negligible excitation of the acceptor

Symmetric depletion of the difference peak centered at zero

Donor-only molecules present

543nm

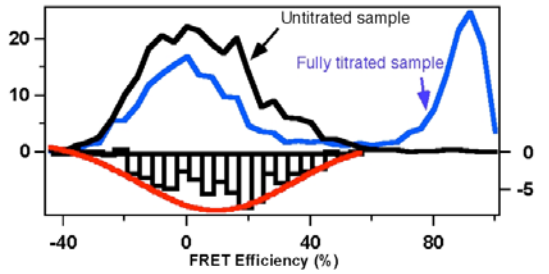

Direct excitation of the donor with small but non-zero excitation of the acceptor

Asymmetric depletion of the difference peak centered at ~ 10%

Double labeled molecules shifted to High ET form

J. Kahn

Decomposing the "zero-transfer" Peak

543nm

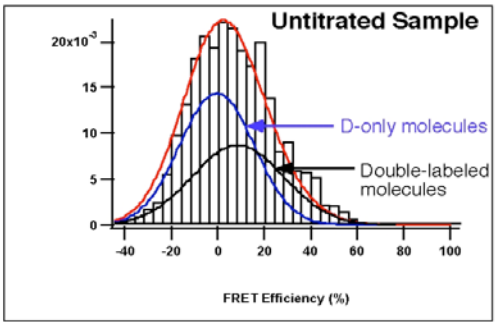

"zero-transfer" peak in the untitrated sample is comprised of 9C14 molecules that have double labeled fully functional fluorophores and molecules that have bleached or missing acceptor fluorophores

543nm

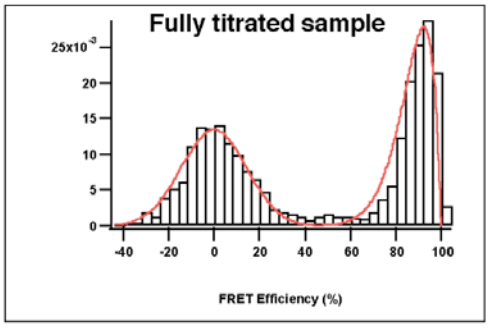

"zero-transfer" peak in the fully titrated sample is comprised of 9C14 molecules that have bleached or missing acceptor fluorophores

J. Kahn

Possible Sources of Discrepancies with Bulk FRET and DNA Cyclization Kinetics

Labeling efficiency

$$E = \left(1 - \frac{I_{DA}}{I_D}\right)\left(\frac{1}{f_A}\right)$$

Calculating ET efficiency by monitoring decreased quantum yield of the donor.

f_A decreases over time as a sample is handled.

- The two ~100 bp tails on the ends of the 9C14 molecule (needed to allow cyclization) could perturb the stabilities of the two different conformers.
- Record's wrapping models? The closed form geometry might be incompatible with surface wrapping.
- Test with SM-FRET on extended constructs - not easy.

J. Kahn

SM-FRET Conclusions

- Single molecule spectroscopy suggests that all of the LacI-bound 9C14 molecules exist as a single closed loop population exhibiting nearly 100% ET. This confirms many of our previous results.
- The extremely efficient energy transfer is consistent only with a loop geometry in which both fluorophores are on the "inside" of a V-shaped repressor, and eliminates the other three possible connectivities. (Zhurkin and Adhya have observed antiparallel loops in related systems.)
- Next steps: immobilization, dynamics with IPTG, application to wild-type loops, open from loops.

J. Kahn

Acknowledgments – LacI

- (Dr.) Michael Morgan
- Dr. Ruchi A. Mehta
- Laurence Edelman
- Raymond Cheong
- Dr. Michael Brenowitz (Albert Einstein)
- Dr. Dorothy Beckett (UMCP)
- Drs. John Harvey and Jay Knutson, NHLBI, NIH

J. Kahn